ABSTRACT

Title of Thesis: PYROLYSIS MODELING AND MATERIAL PROPERTY VALIDATION WITH FLAME HEAT FEEDBACK MODEL APPLICATION

Deepanshu Kishan Bhatia, Master of Science, 2021

Thesis Directed By: Professor James A. Milke, Department Chair
Department of Fire Protection Engineering

Dr. Mark B. McKinnon, Research Engineer
UL Firefighters Safety Research Institute

Materials used in the built environment specially in upholstered furniture in business and residential occupancies act as primary fuel load in fires. This is a cause of concern not only for the building developers but for fire investigators, fire researchers and fire modelers. NIJ Technology Working Group's Operational Requirements for Fire and Arson Investigation have laid out research needs with respect to knowledge of the thermo-physical properties of materials that are common in the built environment. To fill the gaps that limit the analysis capability of fire investigators and engineers, one of the requirement outlined is of adequate material property data inputs for fire modeling as well as fire model validation.

The objectives of this study are to measure thermo-physical material properties of five materials viz. polyurethane foam, polyester batting, polyester fabric, medium density fiberboard and oriented strand board that are used in the built environment. Subsequently using the properties, model the response of these

materials to fire using the condensed phase solver in the numerical solver Fire Dynamics Simulator (FDS) developed by National Institute of Standards and Technology (NIST) with flame heat feedback application. Heat flow meter (HFM) and Integrating sphere were utilized to measure thermal conductivities and emissivity values for the materials. Thermogravimetric Analysis (TGA), Differential Scanning Calorimetry (DSC), Microscale Combustion Calorimetry (MCC) tests were carried out to develop a pyrolysis model and present reaction mechanism. Kinetic parameters were determined using inverse analysis with the Kinetics Neo (NETZSCH GmbH) software and the properties were used to populate the one-dimensional cone model. Flame heat feedback was applied to the model to determine the suitability of model to predict the heat release rate and compared against the cone calorimeter test data.

PYROLYSIS MODELING AND MATERIAL PROPERTY VALIDATION WITH FLAME HEAT FEEDBACK MODEL APPLICATION

by

Deepanshu Kishan Bhatia

Thesis submitted to the Faculty of the Graduate School of the
University of Maryland, College Park, in partial fulfillment
of the requirements for the degree of
Master of Science
2021

Advisory Committee:
Professor James A. Milke, PhD., Chair
Professor Arnaud Trouvé, PhD.
Mark Mckinnon, PhD. UL FSRI

Acknowledgements

This work wouldn't have been possible without the help of lot of individuals. I am grateful to Dr. Steve Kerber and Dr. Daniel Madrzykowski to accept my request and allow me to work in the state of the art UL FSRI lab at Columbia, MD. I would like to express my deepest and immense gratitude to Dr. Mark McKinnon and Dr. Matthew DiDomizio, the two wizards in the lab that made it possible to not only conduct the experiments but do that in the short time frame. I also thank them for their guidance throughout this project and for a fun easy time in the lab.

I would also like to express my sincere and deep gratitude to Dr. James Milke for his support throughout my time at the university and the department with his advice and his consideration to provide me with the assistantship in the department. This allowed me to focus on my studies unhindered by any issues. Dr. Milke's support was crucial in bringing the quality of this thesis work several notches up.

Next, I would like to thank Dr. Arnaud Trouve, for being on the defense committee, for his advice to improve this work and for his advice throughout the 2 years while selecting courses that imparted knowledge and deep understanding about multiple aspects of Fire Protection Engineering.

I would also like to thank my friends in the department, Dushyant Chaudhari and Hongen Zhou who not only took time to discuss what I was doing but also

explained in detail what they did. Dushyant's knowledge and point of view made it possible to assess the results in a different light and incorporate the findings in this study.

Finally, I would like to thank my family for their support and confidence in my abilities to enroll in and complete the program. I would like to remember my late father whose confidence in my abilities, decision making combined with his valuable life lessons and teachings, pushed me to work hard towards successfully completing the program. I would also like to thank all my friends specially Ruth Farington who gave me crucial moral support from time to time and helped me think through things during my times of confusion.

Table of Contents

List of Tables

List of Figures

Chapter 1: Introduction

1.1 Background & Motivation

In 2017, there were 1.3 million fires in the US in which approximately 3655 people lost their lives, and 15,200 people were injured. The estimated cost of direct losses from these fire incidents was $25.6 billion. Out of these, about 39% of fires were reported to be in residential and non-residential buildings accounting for 81% of fire deaths and 84% of injuries [1].

To account for these losses, multiple agencies/organizations can get involved either for litigation, criminal lawsuits or for policy changes to address a community's fire problems. Fire investigations involve analyses conducted in the aftermath of fire occurrences to establish the origin and cause of unwanted fires. Currently there is an absence of a consolidated and comprehensive property data base in the field of fire investigation which was recognized in a white paper released in 2002 by Fire Protection Research Foundation Advisory Council on Post-Fire Analysis. The paper emphasized the need of end-use configuration fire test data of products in a burning rate database to better understand the materials found at fire scenes [2].

Fire being an exothermic combustion reaction involves 4 vital components i.e., fuel, oxygen, heat, and a chemical chain reaction. The fuel here is a substance made up of various mixtures of the elements found in the periodic table, thereby

involving chemistry. Each fuel has a particular tendency to start and sustain a fire that is dependent on the physical and chemical properties of the substance. Knowledge of the materials properties of fuels are essential to study the physics and chemistry of fire.

The Society of Fire Protection Engineers (SFPE) conducted a survey of the fire community in 2016 to identify research needs in fire protection engineering and a web-based library or a material test data database was found as the major response. They identified the need for material properties and testing data and archiving of these data as a part of fire dynamics, investigations, and building fire research priorities in their research roadmap in 2018 [3].

Many material properties are listed in traditional sources such as the Ignition Handbook [4], NFPA Fire Protection Handbook [5] and SFPE Handbook of Fire Protection Engineering [6]. But most of the data does not provide confidence to the fire modelers since much of this data does not include the contextual information which may be important for accurate modeling of fire scenarios [7]. Additionally, there are other existing property databases such as Fire Data Management System (FDMS) developed by National Institute of Standards and Technology and the UK Fire Research Station, NIST Chemistry WebBook, SP Swedish National Testing & Research Institute's open access online database and data created and published under the project titled "The Creation of a Thermal Properties Database" undertaken by National Center for Forensic Science at the University of Central Florida in collaboration with University of Maryland College Park and funded by

the U.S. National Institute of Justice. While some data in these resources are useful, much of the presented data are of limited use for the investigators and model developers due to the data being either of pure substances which are not encountered in usual fire scenarios, absence of images of test articles resulting in vague labels, and much of the data being from products and studies that are two to four decades old. Since these measurements were made and these resources were published, the built environment has developed and evolved, making much of the data in existing resource irrelevant today [7].

To aid fire investigators and driven by a need for properties of materials currently used in the built environment, the NIJ's Forensic Science Research and Development Technology Working Group's Fire & Arson Investigation discipline have funded a project whereby the UL Firefighter Safety Research Institute will directly measure the properties of many common materials and develop a database of the measured properties. The database will function as a tool for fire investigators to evaluate the effects of fuel characteristics on the growth and spread of fire. This data needs to be validated against the additional experimental data to instill confidence in the database. Additionally, it also needs to be seen if the data is good enough for use in computational modelling of a full-scale fire scenario, which will be beneficial for the investigators and model developers to test their theories and hypothesis.

The scope of this study is based on five materials that include polyurethane foam (PU Foam), polyester batting (PET BAT), polyester fabric (PET FAB),

medium density fiberboard (MDF) and oriented strand board (OSB), materials which are commonly used in products encountered in the built environment for the database. A detailed objective of this study is presented in section 1.3.

1.2 Previous Work

1.2.1 Polyurethane Foam

Polyurethane foam (PU Foam) is a part of the diverse polyurethane family of polymers which have a wide range of application in the daily life. PU foam is a polymer which has a urethane bond (-NH-COO-) repeating unit that are developed by reacting alcohols and isocyanates which are products of crude oil. Commonly used raw materials also include polyols, diisocyanates, polyethers and polyesthers [8]. Additives and blowing agents are also used sometimes to enhance the quality of foam depending on the usage. PU foams used in the built environment are flexible, easily moldable, and have little effect of creep so they can retain their shape for a long time, which is why they dominate in the mattress, furniture, and interior industry.

With so many uses in the industry and daily life, pyrolysis of PU foam has been of interest over the past 30-40 years. Environmental researchers have studied the role that polymers play in the environment [9]. Material and chemical engineers have studied the thermal degradation of foams with fire retardant additives [8][10][11]. Chemical and mechanical engineers have studied the kinetics of

thermal decomposition of the foam [12][13][14][15] and fire researchers have conducted research to simulate fire spread on polyurethane foam [16].

Chattopadhyay et al. [8] examined the thermal stability and flame retardancy of polyurethanes. They conducted experiments such as Thermogravimetric Analysis (TGA), Thermogravimetric Analysis - Mass Spectroscopy (TGA-MS) and Thermogravimetric Analysis – Fourier Transform Infrared Spectroscopy (TGA-FTIR) to outline the decomposition mechanism and kinetics of variations of polyurethane. They provided an insight on how the PUs are made of hard segments (HS) and soft segments (SS). A general thermal degradation mechanism of PU was provided as a two to three step process in which the first step was degradation of the HS and the subsequent formation of isocyanate, alcohol, primary or secondary amine and olefin and carbon dioxide. The second and third steps were connected to the decomposition of SS.

Wang et al. [10] studied the thermal degradation behavior and flammability of polyurethanes that were synthesized with flame retardants. A two-step polymerization was carried out to create the material for testing and the tests were conducted in the Thermogravimetric Analysis (TGA) using a coupled Fourier Transform Infrared (FTIR) Spectroscopy. The relationship between the weight loss fraction/degree of conversion (α) and the activation energy (E_a) was determined using the Ozawa method which is an isoconversional method for nonisothermal data where for a fixed degree of conversion (α) the plot of β vs $1/T$ is obtained from thermograms recorded at several heating rates [6]. Although TGA analysis was

done but the study only suggested a two-step degradation behavior for neat polyurethane and polyurethanes modified with flame retardants. The only effect of adding flame retardants was an accelerated thermal degradation and increased char yield.

Rogers et al. [12] undertook kinetic studies on the decomposition of flexible polyurethane foam by conducting TGA experiments in a nitrogen environment. They provided a general two-step reaction mechanism for pyrolysis. The authors of the study compared the difference between a consecutive reaction mechanism and a parallel reaction mechanism and found them to be similar. A general approach for the derivation of kinetic parameters was presented through the study using another study by Criado et al. The authors also compared experimental and theoretical TGA curves, which showed a good fit.

Bilbao et al. [13] conducted a similar study as Rogers et al. where they presented a study of weight loss of the material for different temperatures and atmospheres. They also determined kinetic equations and analyzed the behavior of polyurethane foam pyrolysis in nitrogen and air atmospheres. The kinetic parameter value comparison was made between isothermal and dynamic experiments and nitrogen and air environments.

Studies by Pau et al. [14] and Garrido et al. [15] performed tests with polyurethane foam, where non-fire retardant and fire-retardant formulations were tested under nitrogen environment by the former and flexible polyurethane foam under three different atmospheres with varying nitrogen and oxygen concentrations

were undertaken by the latter. Both studies aimed at determination of kinetic models of pyrolysis. For studies utilizing a nitrogen environment both reached a common conclusion of a two-step reaction model. Pau et al. [15] evaluated the kinetic properties using three graphical techniques of model free method, Arrhenius plot method and inflection point methods in which the first provides result for global kinetic properties for all experiments and the last two are experiment specific. The study suggests that the determination of kinetic parameters from the model free methods is difficult as the parameters obtained are based on a degree of conversion and although provide insight of the mechanism do not provide concrete data to use in pyrolysis models.

Prasad et al. [16] used the Fire Dynamics Simulator (FDS) to numerically simulate the fire spread on polyurethane foam slabs. They conducted small scale experiments such as Thermogravimetric Analysis (TGA) and Pyrolysis Combustion Flow Calorimeter (PCFC) to estimate material properties. The kinetic parameters were found using the TG data and Genetic Algorithms. Arrhenius type reaction rate parameters were fitted using GPYRO software for a two-step reaction mechanism. Cone calorimeter tests were also conducted at flux levels ranging from 20 kW m^{-2} to 50 kW m^{-2} to measure the heat release rate as a function of time. The two-step reaction suggested in this study was recorded for the cone calorimeter tests, where it was observed that one-third of the mass was lost in the first stage and subsequently a liquid melt layer is left. Second stage releases an abrupt amount of energy which is then followed by a decay phase.

To populate the model with the thermo-physical properties, the density was measured using the dimensions and mass of the sample. Thermal conductivity and specific heat values were obtained from the literature rather than measuring them. Emissivity and absorption coefficient data was also considered from the literature.

Four pyrolysis models were developed where in the first model heat release rate data from the cone experiments were directly applied to the model and no user input was required for specifying reaction kinetics data. However, this model was prone to errors in a scenario where the object was the part of a burning building due to the computed burning rate being independent of the external flux incident on the surface of the material. In the second model, solid phase reaction parameters are specified and is assumed that a single reaction controls the burning rate. This model lacked the capability to mimic the TGA & Cone data of two-step reaction. For the third model, to capture the two-step process, the decomposition was modeled as two-step reaction releasing toluene diisocyanate (TDI) and polyols. This model required the Arrhenius kinetic parameters, heats of gasification and combustion and the thermo-physical data to capture the two-step process. The FDS version was not capable of handling multiphase behavior of simultaneous collapse and release of TDI and hence the collapse observed in the cone testing was not captured and the model contradicted the observations made in TGA and cone calorimeter data. The fourth model was built on the shortcomings of model 3 and a three-layer foam slab was considered with layered thermal properties. The top one-third layer mimicked foam properties producing TDI, the second layer of polyols and the third layer of

non-reacting gypsum board. All the models were used to simulate one-dimensional cone experiment. A point to note in this study was the use of an additional 40 kW m^{-2} flux application over and above the cone flux to simulate flame flux since the gas phase in FDS was not invoked. Only model 4 was able to closely replicate the two-stage behavior and hence the same was considered for flame spread simulations.

1.2.2 Polyester Batting & Polyester Fabric

Polyester is the family of polymers which have an ester functional group in the repeating units of the polymer. Polyethylene terephthalate (PET) is the most common type of thermoplastic polyester that is found in the built environment and used as a fiber in clothing, as container for storage of foods and liquids and in combination with glass to create resins, where it is termed as polyester for the former use and termed PET for the latter two uses. Despite a large market presence polyester has not been studied to a great extent with regards to its upholstery application. However, chemical researchers have studied the thermal degradation of PET blends, PET waste and pyrolysis modeling of PET [17][18][19][20], in textile to study the stability of polyester fabric with polyacrylic coating [21] and fire protection researchers to study the decomposition kinetics role in the pyrolysis model [22].

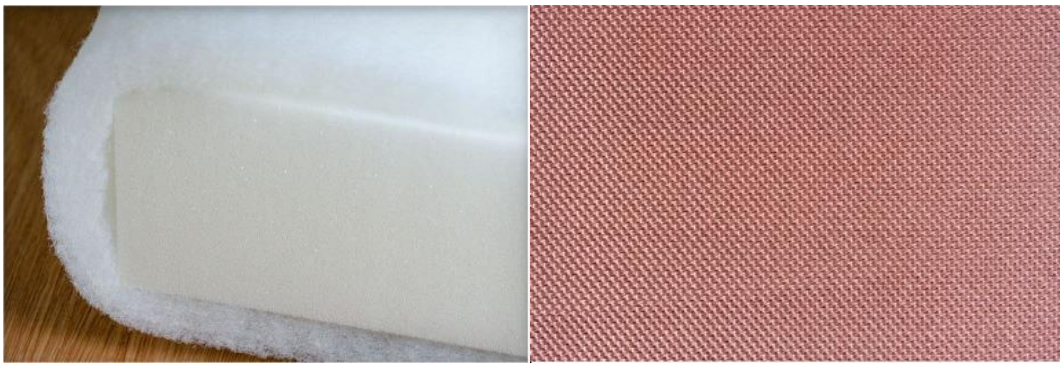

Figure 1.1 Polyester batting on PU foam (left) and zoomed in polyester fabric (right) [23][24]

Martin-Gullon et al. [17] conducted a study to determine the kinetic model for the pyrolysis and combustion of PET. TGA tests were conducted on the PET samples at different heating rates under Nitrogen and Air environments. A pseudomechanism model of pyrolysis was interpreted using 2 independent reactions. The tested material had an initial random scission and divided into carboxyl and vinyl ester group, which it was then proposed to be forming many different gaseous substances that may keep reacting amongst themselves. It was determined that the first reaction is responsible for 80% of the weight loss and the second one is responsible for 6% weight loss which continues. Since it was not possible to distinguish between the combustion reaction step of first part and the second part in the oxygen environment, a simplified series reaction model was proposed which constituted of two consecutive reactions. It is to be noted that the PET for this study was obtained from the beverage PET bottles.

Das et al. [18] undertook the study of thermal degradation of waste PET under inert and oxidative environments. TGA analysis was carried out for PET samples at multiple heating rates in inert and air environment. Kinetic analysis was

done to find the kinetic triplet values; however, no reaction mechanism was provided, nor was a pyrolysis model proposed. Single set of kinetic triplet values for each of the four reaction models were found and the best reaction model was determined.

Girija et al. [19] studied the thermal degradation of various waste PET blends and the effects of different additives in PET on thermal degradation and mechanical properties. TGA experiments were carried out however no reaction kinetics were specified. Citing prior literature, it was determined that the thermal degradation of PET was initiated by chain scission of the ester-linkage which yielded carboxyl and vinyl ester groups. Additionally, the PET blends were studied for change in thermal degradation in the TGA and a set of kinetic parameters were determined for a global reaction for all the blends.

Yang et al. [20] used the first derivative of the TGA (DTG) curve fitting method to determine the apparent kinetic parameters of thermal decomposition of several polymers one of which was PET. The main purpose of this study was to present a graphical user interface (GUI) based software to predict kinetic parameters of the polymers that were studied. The study presented kinetic parameters generated through a software for a global reaction using TGA data but did not provide an individual kinetic reaction mechanism of any of the materials.

Lautenberger et al. [22] conducted a study on fire retardant polyester composites and fitted a three-step nth order reaction, a three-step autocatalytic reaction and a single step reaction to the mass loss rate (MLR) curve obtained from the Fire Propagation Apparatus. The three-step nth order reaction and three-step autocatalytic reaction models provided similar results and estimated closely the first peak correctly but overestimated the second peak by about 8 g m^{-2} s^{-1} (figure 1.2). The single step reaction model almost estimated the first peak and overestimated the second peak in MLR and shifted the second peak in a later time. In this study the polyester was reinforced with glass fiber for which they predicted a three-step reaction model.

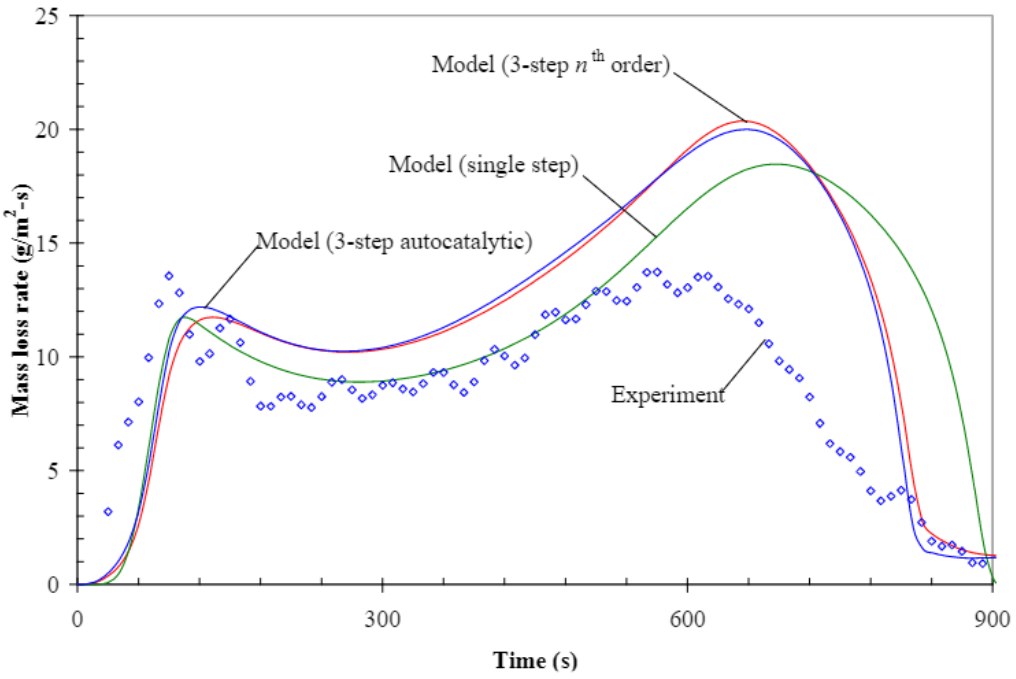

Figure 1.2 Comparison of measured and modeled MLR in FPA for three different kinetic models [22].

1.2.3 Medium Density Fiberboard and Oriented Strand Board

Medium Density Fiberboard (MDF) and Oriented Strand Board (OSB) are engineered wood products (EWP) that have varied and wide use in the built environment. Being cost efficient, these materials find usage in designing the interiors of a building and to make furniture. The mechanical strength and good performance of these materials are particularly important in building construction.

Figure 1.3 Polyester batting on PU foam (left) and zoomed in polyester fabric (right) [25][26]

MDF is manufactured by binding wood fibers with wax or resin under high temperature and pressure conditions [27]. OSB panel is made of strands of woods that are compressed and bound together by adhesive. Due to its mechanical properties, it is widely used in the construction industry for load-bearing applications in walls, and for roofing [28]. Being a wood product, they become a risk for fire in the built environment and hence the study of their thermal properties and degradation mechanism is important. MDF has been studied by many researchers across various branches of science, but mainly the thermal degradation

and kinetic study has been of great interest for fire researchers [27][29][30] and chemical engineers [31]. OSB, with its up-and-coming dominating market share in engineered wood products, is becoming a material of interest for fire researchers [32][33].

Vermesi et al. [27] conducted a study on the one-dimensional model of pyrolysis and ignition of MDF which was subjected to transient irradiation. This study was conducted jointly with FM global to show good agreement of the pyrolysis model to fire propagation apparatus (FPA) experiments. In this experimentation instead of constant irradiation, transient irradiation was considered as it was believed to depict a more comprehensive fire case. The pyrolysis model for this study was taken from a prior study by Li et al. [29] and the kinetics scheme for their one-dimensional model was used from this study. The density was measured while the rest of the thermo-mechanical properties were taken from literature. The model set-up was used to investigate the influence of temperature dependent k and c_p which showed an 18% over prediction in the surface temperature but negligible change in the MLR. When a drying step was added to the reaction scheme it was found that it significantly overpredicted the surface temperature by 78% and changed the behavior of the MLR curve significantly.

Li et al. [29] proposed a four-step parallel reaction pyrolysis model for MDF. They studied in detail the pyrolysis behavior of the samples in nitrogen environment and applied Kissinger's method of finding the possible range of kinetic parameters from second derivative of the TGA (DDTG) curves. These

ranges were used in the GA curve to accelerate the optimization of the inverse method of finding the kinetic parameters. They were able to use the optimized kinetic parameters in their pyrolysis model and provided an overall good fit to the experimental data and overestimated some TGA data while working with optimization of the reaction order. They worked only with TGA data and did not include other bench scale test for validation.

Fateh et al [30]. did some TGA-FTIR study on thermal degradation of plywood under nitrogen and air atmosphere. They did not consider the thermal degradation of wood to happen for different individual components of wood as suggested by Li et al. [29] rather considered the whole material because all the individual components were linked together which is of significance when the individual component mass fraction is not known. They provided a three-step consecutive reaction mechanism using which they demonstrated a good fit to the experimental data.

Gong et al. [33] developed a pyrolysis model for OSB using the literature cited above and provided a four-step consecutive reaction mechanism. They conducted bench scale tests and used inverse modeling techniques to determine the kinetic parameters. The pyrolysis model developed at one heating rate (10 K/min) had a good fit to the experimental data of different heating rates (3 K/min & 20 K/min).

Yuen et al. [34] developed a pyrolysis model and used the model to validate the cone FDS model with the experimental cone data for plywood and particle

board. The conducted cone tests at 3 heat flux of 30-, 40- and 50-kW m^{-2}. They used the gas phase modelling to model cone calorimeter in FDS and used that for study. Mesh sizes of 2 mm, 1.5 mm and 1 mm were used to simulate the FDS model. Although they were able to capture the peak HRR from their FDS results for furniture plywood, the peak was shifted earlier in time from the experimental data. The total heat release obtained from the FDS model was also less than the experimental data. For particle board, they were able to match the FDS output to the experimental data, albeit overestimating the peak heat release rate, they could not get a good fit towards the end of the HRR curve and underestimated the extinction by almost 40 – 80 seconds against the cone test times of 250 – 300 seconds. While their study had good results, the methodology to invoke gas phase and increasing computational time, thereby affecting the economics was not promising enough.

1.3 Objectives & Approach

As part of requirement of a larger project, the first objective of this work was to measure the thermal properties of the five materials in the scope of this project using experimental testing. The thermal properties, along with being used in the database, are used to develop computational model for the cone calorimeter test. The model works in the condensed phase only thereby saving on the crucial computational expenditure and resources which will benefit groups that cannot make those investments.

To populate the FDS model, the inputs required were physical parameters of density, temperature dependent heat capacity and temperature dependent thermal conductivity; reaction kinetics and kinetic parameters; and thermodynamic properties of heat of reaction and heat of combustion. Milligram scale testing on Simultaneous Thermal Analyzer (STA) and Microscale Combustion Calorimetry (MCC) was conducted on the materials for development of the pyrolysis model and determining the kinetic parameters, heat of reaction and heat of combustion. The reaction kinetics and kinetic parameters were determined using the generalized inverse modelling approach [35][36] where a reaction mechanism is determined and pyrolysis model for the five materials is developed. An inverse modeling technique was utilized to determine the kinetic parameters of Activation Energy *(E_a)*, Arrhenius Constant *(A)* and reaction order *(n)*. The inverse modeling was conducted on Kinetics Neo software by NETZSCH GmbH where the kinetic parameters were determined out of the various methods/functions present in the software. The specific heat and thermal conductivity were determined using the heat flow meter apparatus. Density of the materials was directly measured using the mass and volume of the specimen.

A reaction mechanism and pyrolysis model for polyester batting and polyester fabric was presented. Although the base fuel of polyethylene terephthalate (PET) has been studied in other forms [18][19][20][22], but PET in the form of polyester batting has not been studied and is essential given its heavy use in the upholstered furnishings.

The thermal properties obtained by the above process were utilized in the 0-D FDS model for milligram scale and the generated curves were compared against the experimental testing curves.

A computational model of the cone calorimeter was developed using FDS v6.7.5, a numerical solver for fire driven fluid flow to perform the condensed phase calculations with specified inputs and boundary conditions, populated from the experimental regimen. Since the gas phase was not invoked, flame heat feedback model developed in a study by McCoy and Tilles [37] was incorporated in the cone model to mimic the real world conditions of heat flux incident on the material surface. Cone calorimeter testing was carried out to provide the data for comparison of the FDS model. The applicability of the flame heat feedback model was investigated on the materials and discussion and improvements were suggested based on the comparison.

Chapter 2: Experimental Methodology

2.1 Materials

2.1.1 Common Preparation

All the samples were cut into 0.2 m x 0.2 m samples of different thicknesses as per the individual requirements mentioned in the subsequent sections, to be used for testing in the heat flow meter and other smaller pieces were used for the milligram scale testing. All the sample pieces were kept in the oven at 378 K for at least 2 days to rid the samples of moisture. Then the samples were kept in the desiccator to cool down before machining and were kept in the desiccator throughout the duration of the testing.

2.1.2 Polyurethane Foam (PU foam)

The PU foam (figure 2.1) obtained at the UL FSRI lab was a part of the larger generic couch cushion found in upholstered furniture, and the cushion included 3 of the 5 materials used in this testing. The couch cushion had a PU foam sandwiched between two layers of polyester batting and covered with polyester fabric. The sample preparation was general as described in section 2.1.1 and size of the PU foam sample for heat flow meter (HFM) measurements was 50 mm. The density of the material measured at room temperature was 30.0 ± 0.56 kg m^{-3}. Milligram scale samples were prepared as described in section 2.2.

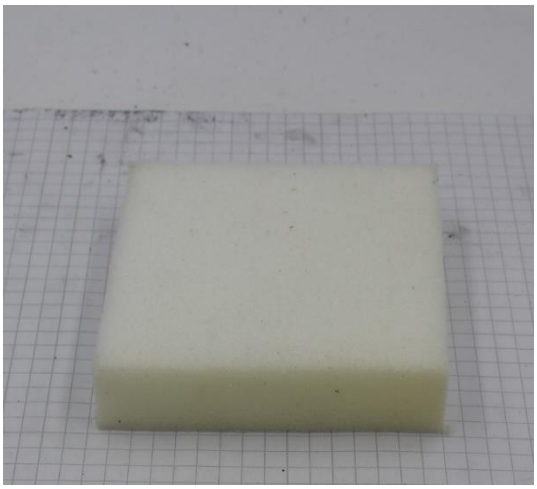

Figure 2.1 PU foam

2.1.3 Polyester Batting (PET Bat)

As mentioned in section 2.1.2, the PET batting was a part of the larger couch cushion. Sample preparation was general as described in section 2.1.1, and the size of the sample was considered as 44 mm for testing the sample in the HFM. The size of the sample was considered in line with the thickness that was used for the cone calorimeter testing. The average density of the material measured at room temperature for the cone samples were 15.00 ± 1.5 kg m^{-3}

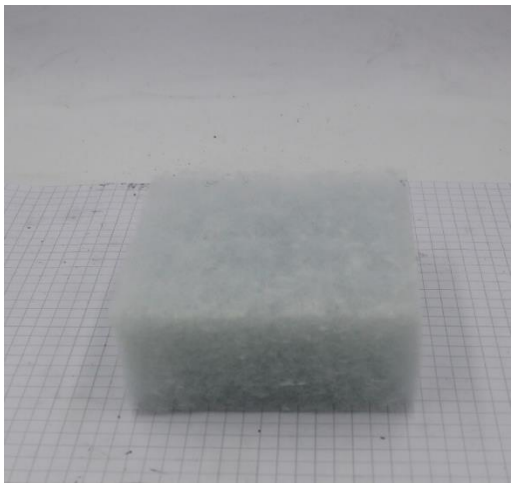

Figure 2.2 Polyester Batting

2.1.3 Polyester Fabric (PET Fab)

As mentioned in section 2.1.2, this PET fabric was a part of the larger couch cushion. Sample preparation was general as described in section 2.1.1, but the thickness of the fabric was 0.47 mm. There were concerns of thickness while using the material for testing in the HFM, but the apparatus had the lower limit for measurement at 0 mm and supported the measurements of thermal conductivity. The density of the material measured at room temperature was 408 ± 10 kg m^{-3}.

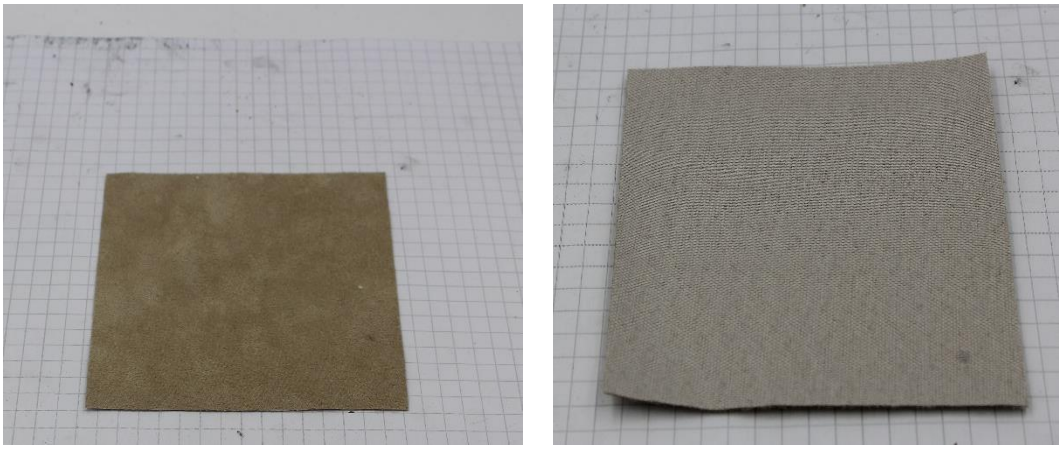

Figure 2.3 Polyester Fabric (front & back respectively)

2.1.4 Medium Density Fiberboard (MDF)

Medium density fiberboard was obtained from UL FSRI for testing. The material was part of MDF panel purchased from Home Depot which is representative of the ones found generally in home construction. Sample preparation was general as described in section 2.1.1, but the thickness of the board

was 19.0 mm. The density of the material measured at room temperature was 736.0 ± 12 kg m^{-3}.

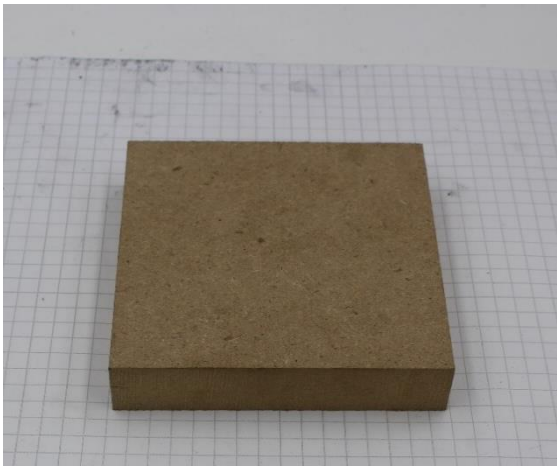

Figure 2.4 Medium Density Fiberboard

2.1.5 Oriented Strand Board (OSB)

The material was part of an OSB panel that was obtained for testing by the UL FSRI lab. The material was purchased from Home Depot and is representative of the OSB found generally in home construction. Sample preparation was general as described in section 2.1.1, but the thickness of the board was 16.0 mm. The density of the material measured at room temperature was 600 ± 36 kg m^{-3}.

Figure 2.5 Oriented Strand Board

2.2 Milligram-scale tests

The microscale testing of the materials was carried out on multiple instruments that catered to different parameters of interest. The instruments work with milligram scale samples and form a basis to provide a wide range of thermal properties. This type of testing is beneficial when the amount of sample collected from the investigated site is of very limited quantity. The samples for these tests were powdered using a cryogenic mill Retsch MM301. The mill powdered the samples evenly with a very fine particle size which helped in even packing of materials in the crucibles for good thermal contact.

2.2.1 Simultaneous Thermal Analysis (STA)

Two types of tests were performed on the STA, these tests were, the thermogravimetric analysis (TGA) and differential scanning calorimetry (DSC) which are conducted simultaneously in the same apparatus. Tests were conducted using a Netzsch 449 F3 Jupiter, shown in figure 2.6. The test was conducted to determine the essential parameters related to reaction kinetics and decomposition thermodynamics. The apparatus consists of two identical platinum-rhodium crucibles, one reference (empty) and another sample filled crucible that were placed in the furnace and exposed to identical temperature program in a nitrogen atmosphere. The crucibles were used with a lid that had a small hole to allow for the escape of pyrolysis gases during the tests.

The evolution of sample mass was measured with the built-in high sensitivity micro-balance and heat flow was measured using thermocouples located below the crucibles. Both the measurements were recorded as a function of temperature and time as the sample is heated up. The STA was calibrated prior to the testing using 6 compounds whose melting temperatures were known and ranged from 341 K to 1082 K. The consideration of sample sizes in these tests is very small i.e., thermally thin. The sample sizes in the tests ranged from 2-5mg. The powdered samples were packed properly in the crucibles to ensure good thermal contact and were exposed to 3 heating rates of 3 K min^{-1}, 10 k min-^{1} and 30 k min^{-1} and were repeated 3 times each.

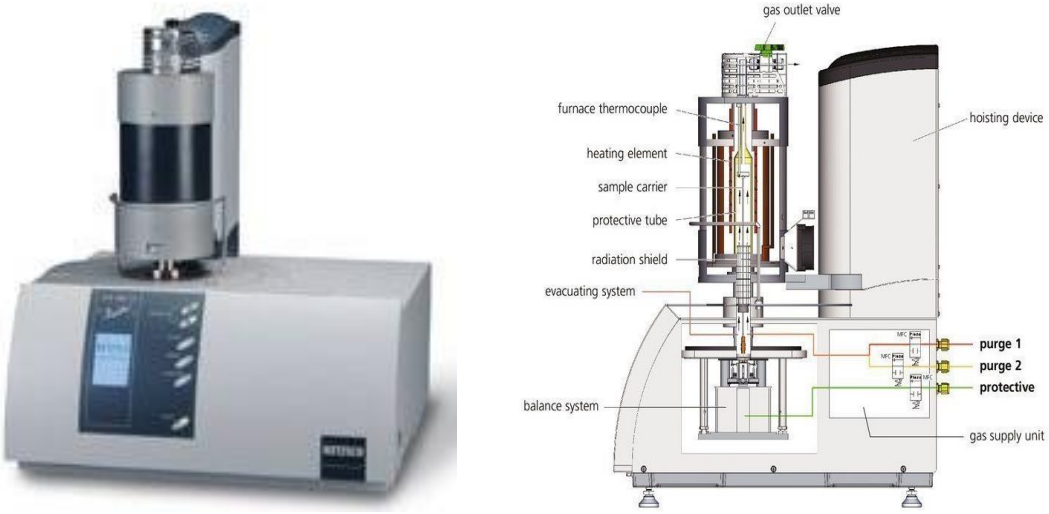

Figure 2.6: STA Instrument [7]

2.2.2 Microscale Combustion Calorimetry (MCC)

Microscale combustion calorimetry testing is conducted to measure the heat of combustion of gaseous pyrolyzates and performed as per the ASTM D7309 – 20 standard [38]. The process includes production of pyrolyzates by a controlled

pyrolysis of the sample in an inert atmosphere that is followed by combustion of pyrolyzates in excess oxygen condition. For this test the crucible with a milligram sample was kept in a furnace without a lid and exposed to the prescribed temperature and anerobic conditions. The gases evolved from the pyrolysis transport from the furnace to a combustor maintained at a high temperature where they mix with excess oxygen and completely combust thereby releasing heat. The time integral of the heat release rate provided the heat of combustion for that material. A detailed description of the MCC can be found elsewhere [39].

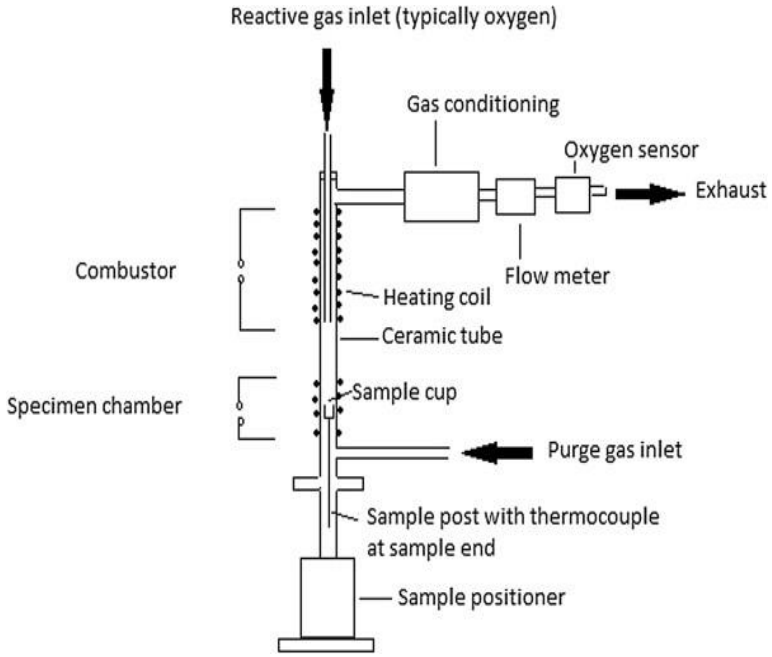

Figure 2.7: MCC Instrument [40]

2.2.3 Heat Flow Meter (HFM)

Heat flow meter (TA instruments - Fox 200 model) was used to find the thermal conductivity k (W m^{-1} K^{-1}) of the materials as a function of temperature and specific heat capacity, C_p (J kg^{-1} K^{-1}), values for temperature up to 50^0C. The

HFM measures for homogenous materials whose dimensions do not change during the measurement and is used as a steady-state method to measure thermal conductivity and volumetric specific heat $C_p \rho$ (J m^{-3} K^{-1}). The instrument works with a parallel faced sample of 0.2 m x 0.2 m dimensions. The maximum thickness of the sample is limited to 50 mm. The instrument has two isothermal flat plates that are maintained at two different temperatures, a cold plate and a hot plate, between which the sample is placed. Calibration of the instrument was done using a standard material of known thermal conductivity to get the calibration factors used as instruments characteristics to perform measurements. For the specific heat capacity, the plates' heat capacity was measured 3 times without a sample and the data was sent to manufacturer who then provided a modified registry file for use in specific heat testing [41]. The principle used in the measurement of thermal conductivity is based on 1-D Fourier law. The heat flux flowing through the sample is measured using the heat flux transducers and the temperature gradient (dT/dx) is calculated by the temperature of the plates. The temperature of the hot and cold plates is varied throughout the measurement to get thermal conductivity values at various temperatures. The test takes several hours to complete since being a steady state test, it needs to ensure the sample attains steady state conditions required for measurement.

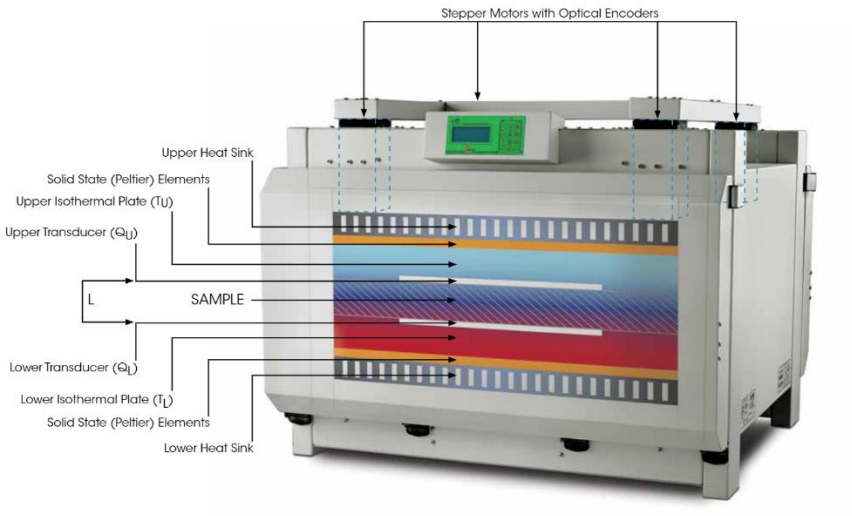

Figure 2.8: Heat flow meter [7]

2.2.4 Integrating sphere spectrophotometer

The emissivity of the samples was directly measured using the integrating sphere apparatus in accordance with ASTM E903 standard [42]. The test is performed on the Fourier Transform Infrared (FTIR) reflectometer equipped with an integrating sphere to measure the reflectance from a sample in a near normal-hemispherical absorptance, reflectance and transmittance of the materials [42][43]. The integrating sphere collects the reflected or transmitted radiation from a sample to the hemisphere. The electromagnetic radiation associated with the sample is captured and the energy is measured by the spectrophotometers on the sphere. The device is useful in the fire science research to measure the emissivity of a wide range of materials with a flat form factor [7]. The measurement technique is elaborated in section 4.2.1. The integrating sphere setup is presented in figure 2.9.

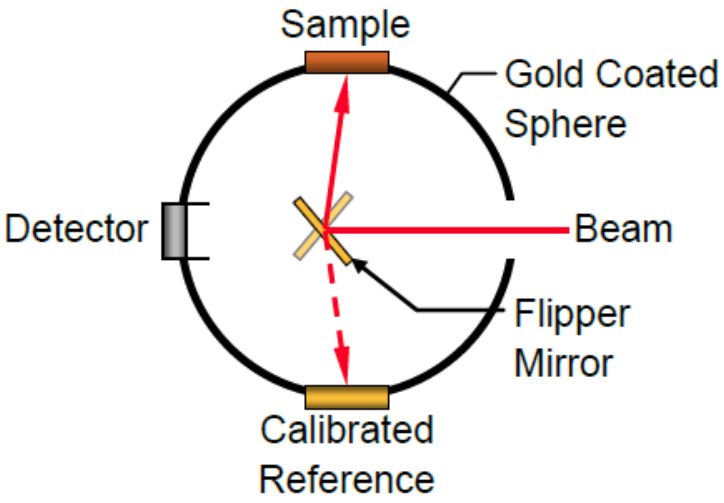

Figure 2.9: Integrating Sphere [7]

Chapter 3: Experimental Results and Discussion

3.1 Milligram-Scale Testing

3.1.1 Mass Loss Rates

The STA experiments for all the materials were conducted for 3 heating rates 3 K/min, 10 K/min and 30 K/min and the experiments were repeated in triplicate at all the 3 heating rates. MCC tests were conducted at one heating rate of 30 K/min and repeated in triplicate. The results from the STA and MCC experiments are as presented in this section for all the materials. The graphs show the averaged normalized total mass data and average mass loss rate data curves from the TGA at each heating rate. The graphs for the average heat release rate and total heat release rate results at 30 K/min and normalized heat flow DSC curve are also presented. For both the STA and MCC tests for all samples there is no peak visible in the 350 - 400 K temperature range since all the samples were dried in the heater before milling and using for tests.

The data obtained from the TGA for the first derivative (DTG) curve was smoothed in the Proteus analysis software that was used to analyze the results of the STA tests. For smoothing, a Savitzky-Golay digital filter was used which was the standard filter in the Proteus software. The smoothing was applied such that the peaks of the DTG curve are not distorted and the max value of the peak is maintained. The observations noted for the materials are discussed in this section.

3.1.1.1 PU foam

For PU foam two distinct peaks are observed in the MLR curve presented in figure 3.1. Not taking into consideration the drying of samples before testing – which would be the first event occurring at around 360-390 K range – the first process is observed in the 550-600 K range for the three heating rates and the second process is observed in the 630-690 K range. The observation of the 2 peaks is consistent with the literature [8][10][12][13][14][15][16] regardless of the material preparation with additives for fire retardation or virgin soft PU foam. The residue generated from the STA testing was between 1.6% to 2.7% of the initial mass. Both processes observed in the STA tests were endothermic which is known through the literature [16][44] to induce production of combustible TDI and polyols in the first process and pyrolysis of polyols in the second stage to produce other combustible gases. Most of the mass loss was observed in the second process as visible in the TGA curve which shows the polyols to be of major concentration in the composition of PU foams. The reaction mechanism observed was for two reactions, however for reasons explained in section 4.2.5, the reaction mechanism chosen for the PU foam samples was a three-reaction mechanism which fit the TGA curve analysis in the analysis software better. Consistent with all the prior studies, the reaction mechanism for the pyrolysis of the PU foam was considered to be a consecutive reaction mechanism in which two intermediate compounds were generated and the last reaction leading to the generation of very little residue given

that PU foam is a non-charring polymer. The reaction mechanism for PU foam is presented in chapter 4.

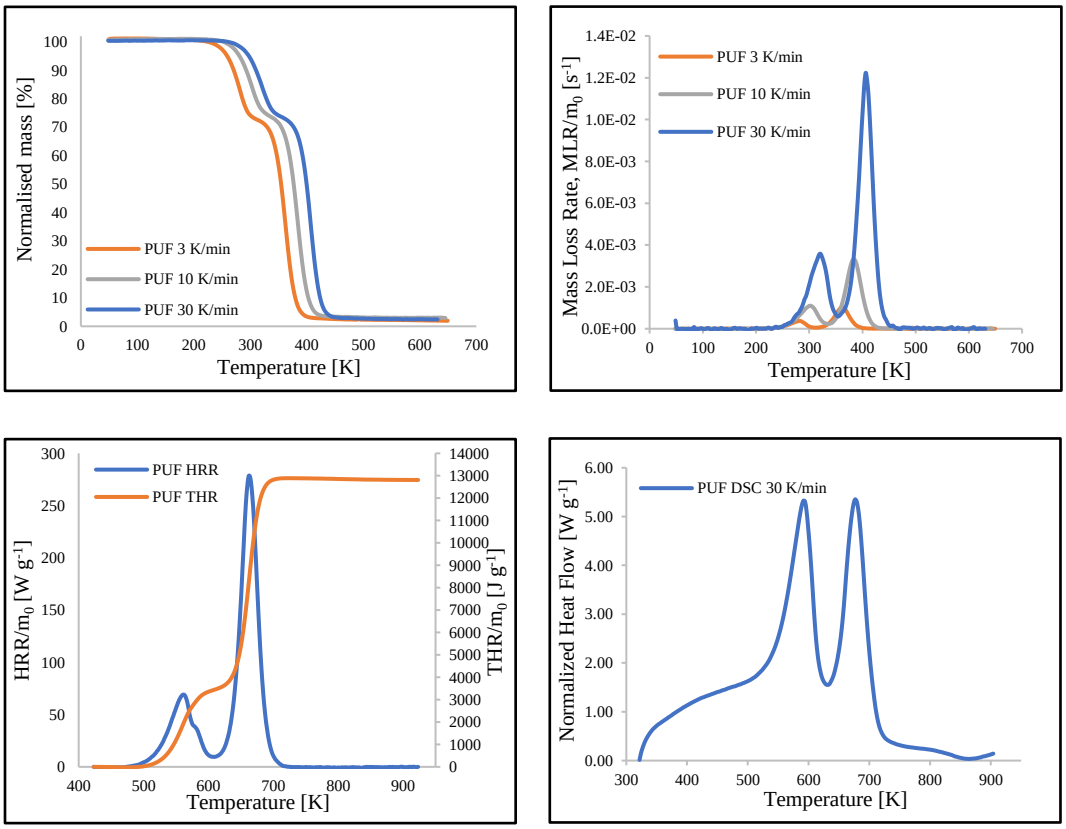

Figure 3.1: Normalized mass curve, Mass loss rate curve, Normalized heat flow curve and Peak and Total heat release curve for PU foam (clockwise-direction)

3.1.1.2 PET Batting

For PET batting, the graphs are presented in figure 3.2. Three distinct processes can be observed during the pyrolysis in the STA. The first peak visible in the STA is around the 530-540 K temperature for the 10 K/min curve that signifies an endothermic process without a change in the MLR curve, which suggests a melting process. The second process occurred at the start of the main peak located at 630-660 K range in the MLR curve, which is verified by the STA curve that shows a process at 650 K in the 30 K/min DSC curve. The third process

which generated peak mass loss is observed at 680-750 K range which preceded the tail that approached zero and leads to char generation which was about 21% of the original mass of the samples tested. The process proposed for polyester batting is consistent with the literature [17]. The different heating rates did not have a marked effect on the char production which was 20.9%, 20.85% and 20.75% for 3 K/min, 10 K/min and 30 K/min respectively. The TGA and DTG curves here do not capture the exact number of processes since the first process is a melting peak of polyester batting between 500-550 K and does not involve mass loss and the other two processes are happening in quick succession which is visible in the DSC curve. The reaction mechanism for the pyrolysis of the polyester batting is detailed in section 4.2.5.

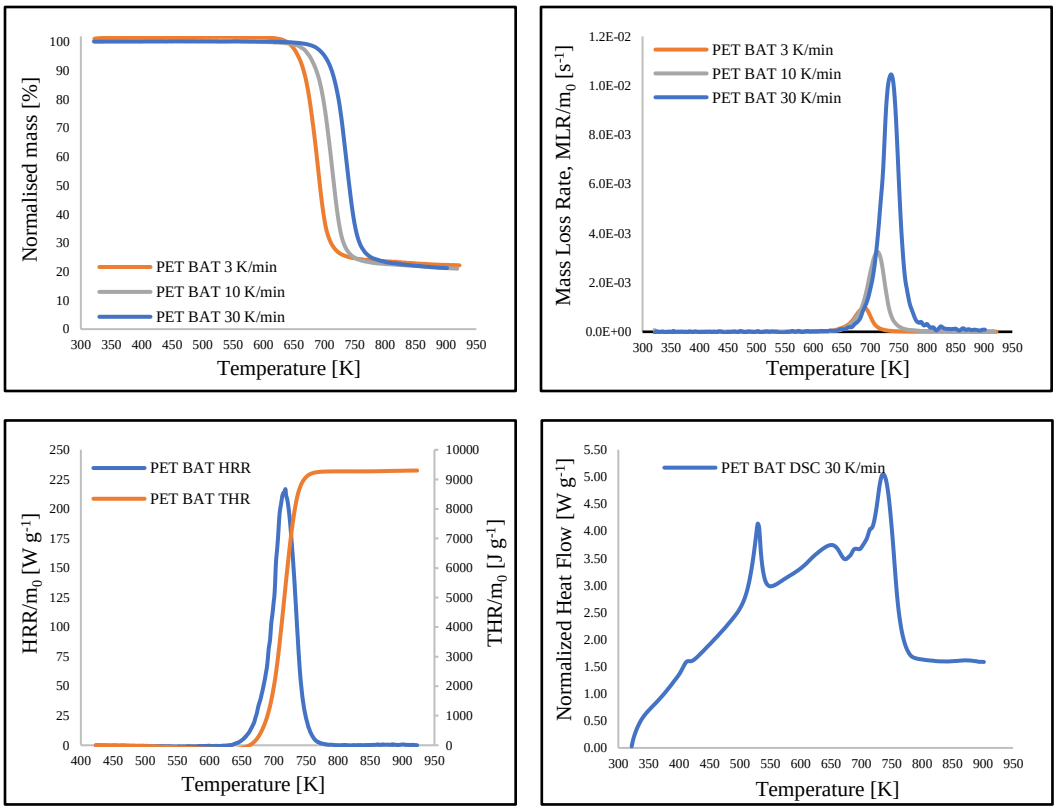

Figure 3.2: Normalized mass curve, Mass loss rate curve, Normalized heat flow curve and Peak and Total heat release curve for PET batting (clockwise-direction)

3.1.1.3 PET Fabric

For PET fabric, the graphs are presented in figure 3.3. Four peaks/distinct processes can be observed in the DSC curve out of which three processes can be observed in the DTG/MLR curve as well. The first peak visible in the DSC curve is that of melting peak observed at 530-540K range suggested by the fact that there are no aberrations on the MLR curve. A second small peak is visible on the DSC as well as the MLR curve in the 600-650 K range suggesting a start of the process with most mass loss in the third process observed from 670-770 K range for the three heating rates. An additional feature is observed at the end of the MLR curves which signify a fourth process which continues until the end of the temperature program that gives an extremely small slope to the tail of the TGA curve. This phenomenon is in line with the observation in the literature [17] where after a major process contributing to majority of mass loss a reaction is identified at the end which continues till the end of the temperature program. The resulting char generation in the sample is about 17.7% with not much variation in the char between heating rates. It can be noted that polyester fabric and polyester batting have similar signals and processes in the STA experiment. This is expected since both the materials are made of similar fuel with different manufacturing techniques that impart a continuing reaction observed in the polyester fabric. The reaction mechanism of the PET fabric pyrolysis process is detailed in section 4.2.5.

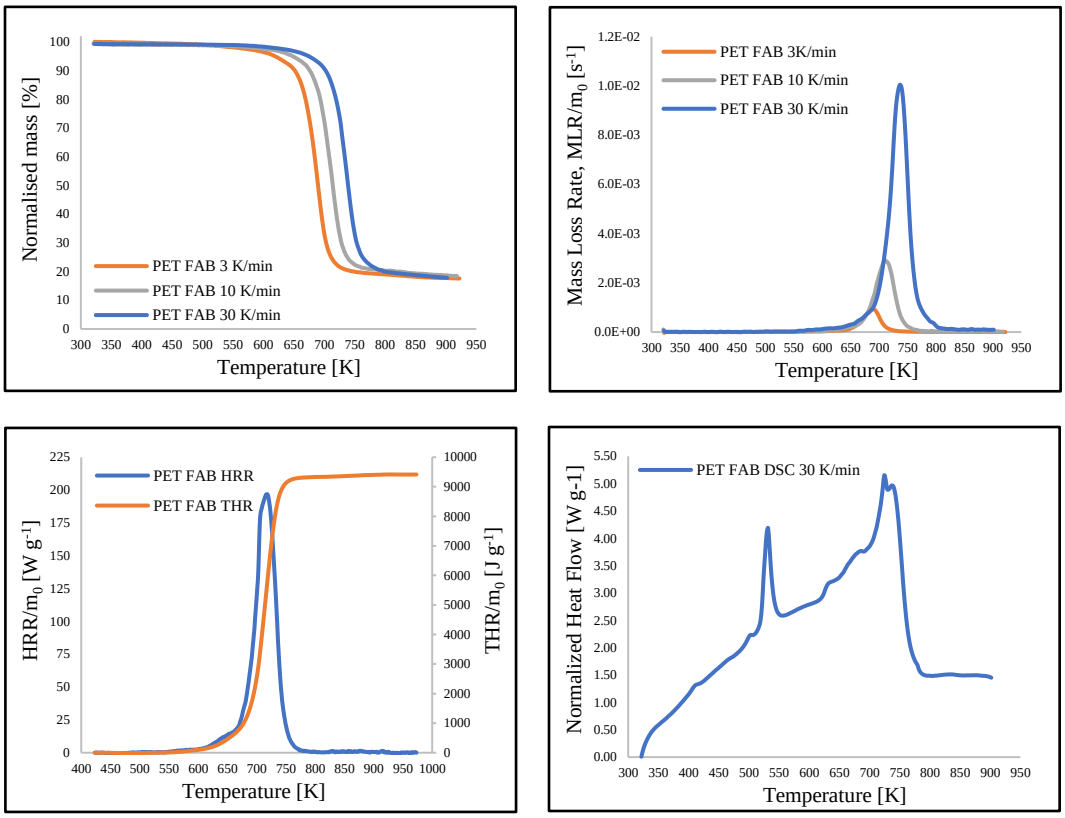

Figure 3.3: Normalized mass curve, Mass loss rate curve, Normalized heat flow curve and Peak and Total heat release curve for PET fabric (clockwise-direction)

3.1.1.4 Medium Density Fiberboard (MDF)

For MDF, as visible from figure 3.4, all the processes were not clearly identifiable even from the DSC curve and had three processes clearly identifiable. However, using technique and approach suggested in the study conducted by Li et al [29] where they use the second derivative of the TGA (DDTG) curve, four processes were observed using the DTG/MLR, DSC and the DDTG curve. While the DTG & DDTG curve provided the number of processes, DSC curve provided the type of processes taking place. It was observed from the DSC curve that three

of the processes were endothermic while the last process was exothermic process which was proposed by Atreya et al [45]. They suggested that after an endothermic pyrolysis process where large mass loss is seen, an exothermic reaction period is observed which results in a small mass loss during this process. The first process was observed at 475-525 K range, the second process was observed from 520-575 K range, the third process was observed from 600-650 K and the final process – which is an exothermic mass loss process – is observed from 625-700 K for the three heating rates. The char production by the samples is in the 21.5% - 23.5%. The pyrolysis reaction mechanism for MDF is detailed in section 4.2.5.

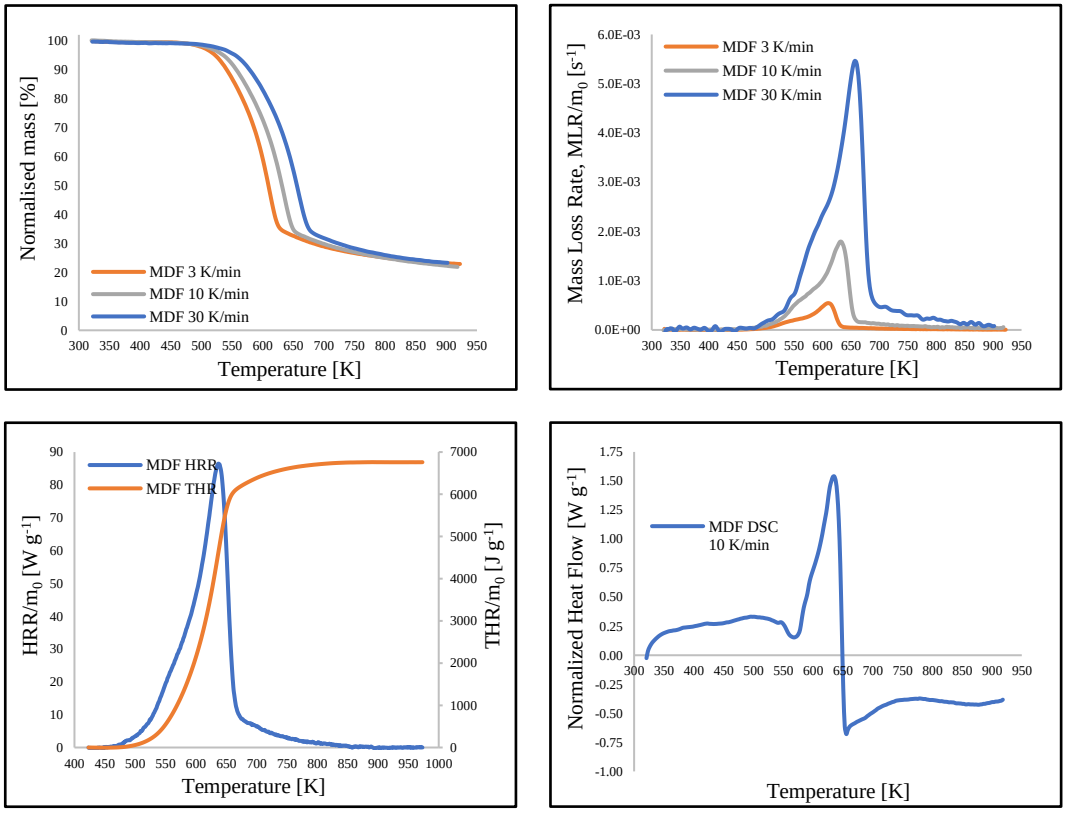

Figure 3.4: Normalized mass curve, Mass loss rate curve, Normalized heat flow curve and Peak and Total heat release curve for MDF (clockwise-direction)

3.1.1.5 Oriented Strand Board (OSB)

Being an engineered wood product similar to MDF, a similar technique was used to identify the processes in the pyrolysis process of OSB. This technique was also supported by the recent study conducted by Gong et al [33] for the same material. The curves associated with OSB are presented in figure 3.5. The four processes were observed in which the first process was located at the left foot of the main peak at 475-550 K range, the second process was the main peak located at 575-625 K range, the third process at the bottom of the main peak 650-725 K range and the final process that was a slow continuing decay phase at 750-800 K range. Out of the 3 processes, the first two processes are endothermic processes, and the last process is exothermic which is in line with the study conducted by Atreya et al [45]. The char production for this sample was in the range of 21.7% - 22.5%. The pyrolysis reaction mechanism for OSB is detailed in section 4.2.5.

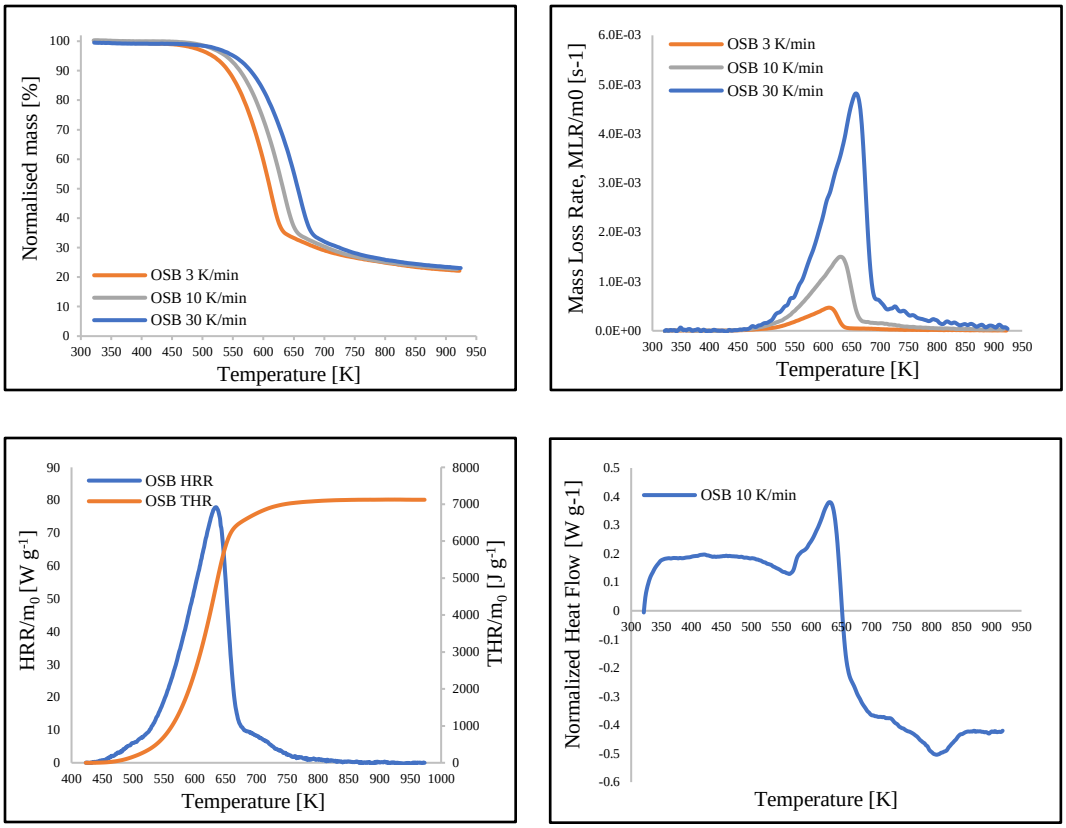

Figure 3.5: Normalized mass curve, Mass loss rate curve, Normalized heat flow curve and Peak and Total heat release curve for OSB (clockwise-direction)

Chapter 4: Computational Framework, Property Determination and Modeling

4.1 Introduction

One of the main objectives of this study is to investigate the correlation of experimental to the simulated cone calorimeter tests using the properties obtained from the bench-scale tests. The modeling was carried out in Fire Dynamics Simulator (FDS) version 6.7.5 developed by NIST. FDS has built-in pyrolysis modeling capabilities using which the milligram scale tests were setup with thermally thin consideration in 0-D and the cone calorimeter was modeled in 1-D. It is assumed that the heat transfer under the cone calorimeter progresses along the thickness of the material and lateral temperature difference is assumed to be negligible. With solid phase solver in the FDS the heat transfer is simplified by solving 1-D calculations, which is why it was preferred to start with rather than opting for the complex 2 and 3-D heat transfer.

4.2 Determination of material properties

To populate the FDS code, properties of the materials were required to be entered into the code. The input parameters to the FDS model for both milligram scale model and cone model were either directly measured or were determined using the experiments conducted on the apparatus mentioned in chapter 2. The material properties that were required in the FDS code are provided in table 4.1.

The details of the measurement techniques are elaborated from section 4.2.1 onwards.

Table 4.1 Material properties' input for FDS models

Sample Properties		Determination Technique
Thermal & physical properties	Emissivity	Integrating sphere
	Density	Measured from sample using volume and mass
	Thermal conductivity, k	HFM
	Specific heat, C_p	HFM
Kinetic parameters	Pre-exponential factor, A	TGA
	Activation energy, E	TGA
	Reaction order, n	TGA
	Product yield	TGA
Thermochemical properties	Heat of reaction	DSC
	Heat of combustion	MCC

4.2.1 Emissivity

The emissivity of the materials was directly measured and calculated using the integrating sphere apparatus for the estimated temperature of each cone test set point for each material using the method outlined in ASTM E903 [42]. This analysis assumes that the materials are opaque to light in the infrared region (no transmission), the sum of reflectivity and absorptivity is equal to unity, and that the absorptivity is equal to the emissivity. The emissivity values for the materials that was considered in the cone model are mentioned in table 4.2.

Table 4.2: Emissivity values of materials at expected temperatures in cone calorimeter testing for each heat flux

Materials	25 kW m^{-2}	50 kW m^{-2}	75 kW m^{-2}
PUF	0.88	0.86	0.84
PET BAT	0.92	0.91	0.90
PET FAB	0.58	0.54	0.52
MDF	0.83	0.80	0.78
OSB	0.86	0.84	0.82

4.2.2 Density

Density of the materials was directly measured using the volumetric technique in which the mass and dimensions of the material were measured before and after drying, and density was computed for different inputs to models. The pre-dried density was considered for the 1-D cone model and the density of post-dried materials was considered for the 0-D TGA model since the testing of the materials on the STA was conducted after drying them in the heater for 2 days to rid the samples of moisture. The absence of moisture was confirmed by the dessicator reading which displayed < 10% on the RH monitor. The FDS model does not allow for a temperature dependent density RAMP convention and hence the density of the intermediates was assigned to the individual reactions.

The densities for intermediates of MDF and OSB were interpolated by considering the reduction of sample mass in each reaction. It was assumed that the thickness of the sample is not changing, and, in each reaction, there was a generation of pyrolysis products which reduced the mass of the remaining sample for the next reaction. Using the mass fraction of the intermediate from last reaction the density of the intermediate was calculated for subsequent reaction assuming constant thickness.

As for the density of the polymers viz. PU foam, PET bat and PET fab, PU foam is a material which tends to change phase after the first reaction [44] and hence the density of the intermediate was considered from the study for the subsequent reactions. Additionally, PU foam tends to leave or very little residue as

it is observed from the TGA curves in section 3.1.1.1. For PET bat and PET fab the material undergoes phase change prior to onset of decomposition which can be seen from the TGA curves provided in section 3.1.1.2 and 3.1.1.3. This phase change prompts consideration of different density which was considered for PET fuel for both the materials [44]. To obtain the density of the virgin material for all the materials, three different samples were measured for each material and the mean density was determined, values for which are provided in section 2.1.

4.2.3 Thermal Conductivity (k)

The thermal conductivity of the materials was measured using the heat flow meter. The HFM can directly measure the conductivity values up to a temperature of 50^0C and the subsequent values were determined by interpolation of the available values by plotting them in the temperature vs thermal conductivity in the x-y plane. It was found that for all materials the 'log' curve fit to the available values better than the linear or a power curve fit, and the thermal conductivity values provided better spread and fit (table 4.3) to the literature data of the references mentioned in this study for different materials. The values were considered in the cone model with a RAMP convention to specify temperature dependent thermal conductivity values.

Table 4.3: Equation of curve fit for thermal conductivity values of all the materials

Material	Fit (k)
MDF	0.1037*LN(T) - 0.4729
OSB	0.1055*LN(T) - 0.4941
PU foam	0.0576*LN(T) - 0.2903
PET Batting	0.1174*LN(T) - 0.6162
PET Fabric	0.0874*LN(T) - 0.4623

4.2.4 Heat Capacity (C_p)

For the specific heat measurement, the value of the volumetric specific heat $C_p\rho$ is calculated as:

$$C_p\rho = (\frac{H}{\Delta T} - H_{HFM})/L$$

Where $\frac{H}{\Delta T}$ is the amount of heat absorbed per unit area per ^{0}C absorbed by the sample, H_{HFM} is the area normalized heat provided by the heat flow meters and is software calculated using coefficients in the registry file and L is the sample thickness [46].

The heat capacity of the materials was directly measured for the materials up to 50^{0}C in the HFM and were used to interpolate the thermal capacities for the intermediate components. Additionally, heat capacity was also calculated at elevated temperatures up to the onset of degradation, from the DSC curve. The DSC

curve was analyzed for a portion before the onset temperature for degradation and the measured heat flow was divided by the instantaneous heating rates to get the value of C_p at different temperatures. The heat capacity of the char for engineered wood products and polymers were assumed to be 1.2. Using the values from the HFM and DSC curve, a curve fitting was conducted to extrapolate the C_p values and develop temperature dependent heat capacity figures. It was found that for all materials the 'log' curve fit to the available values better than the linear or a power curve fit (table 4.4) and the specific heat values provided better spread and fit to the literature data of the references mentioned in this study for different materials. The data was extrapolated with an increasing trend up to the onset temperature and thereafter a decreasing trend up to the char C_p values. These extrapolated values for intermediate components in pyrolysis process were used in the model with RAMP convention to specify temperature dependent thermal conductivity values.

Table 4.4: Equation of curve fit for specific heat values of all the materials

Material	**Fit (C_p) (Till onset)**
MDF	900.48*LN(T) - 3902.7
OSB	1151.4*LN(T) - 5364.3
PU foam	1892.6*LN(T) - 8957.8
PET Batting	2450.8*LN(T) - 12684
PET Fabric	227.98*LN(T) - 411.73

4.2.5 Kinetic Parameters (A, E_a, n & Stoichiometry):

Thermogravimetric analysis is a generalized tool that is used to study the pyrolysis of the fuels present in the materials. TGA data was used to determine the different fractions of components generated along with their reaction kinetics. For each of the reactions hypothesized, the kinetic triplet values of pre-exponential factor, activation energies and reaction orders, and the contribution of each reaction were determined from the TGA normalized mass curve using a reverse curve fitting and optimization methodology. The methodology was applied using a kinetic analysis software 'Kinetics NEO' developed by NETZSCH GmbH for establishing kinetic parameters. The software provides Model-Free (isoconversional) analysis as well as Model-based kinetic analysis scheme. The model free (isoconversional) analysis is based on a representation of the pyrolysis process through a single-step global kinetic reaction. This analysis evaluates the kinetic parameters at different values of degree of conversion, α. The form used in the isoconversional method is [6]:

$$\frac{d\alpha}{dt} = A(\alpha) \cdot exp\left[-\frac{E_a(\alpha)}{RT}\right] \cdot f(\alpha) \tag{4.1}$$

which is the isoconversional form of the basic rate equation represented as [6]:

$$\frac{d\alpha}{dt} = A \cdot exp\left[-\frac{E_a}{RT}\right] \cdot f(\alpha) \tag{4.2}$$

where $\frac{d\alpha}{dt}$ is the extent of conversion with respect to time, A is the pre-exponential constant, E_a is the activation energy and $f(\alpha)$ is the mathematical function that describes the reaction model. The $A(\alpha)$ and $E_a(\alpha)$ are the conversion dependent pre-exponential constant and activation energy, respectively (α =0.1, 0.2……. 0.9). The model free method represents the activation energy and pre-exponential constant as continuously changing with the progress of the reaction. Though the model free analysis provides information regarding the number of reactions according to the change in slope of the activation energy and pre-exponential isoconversional plot, it does not give any information about the features of the reaction including the contribution of each reaction in the pyrolysis process. It also provides a global kinetic triplet of parameters which are not unique to the individual reactions and proves difficult to be applied to a pyrolysis model.

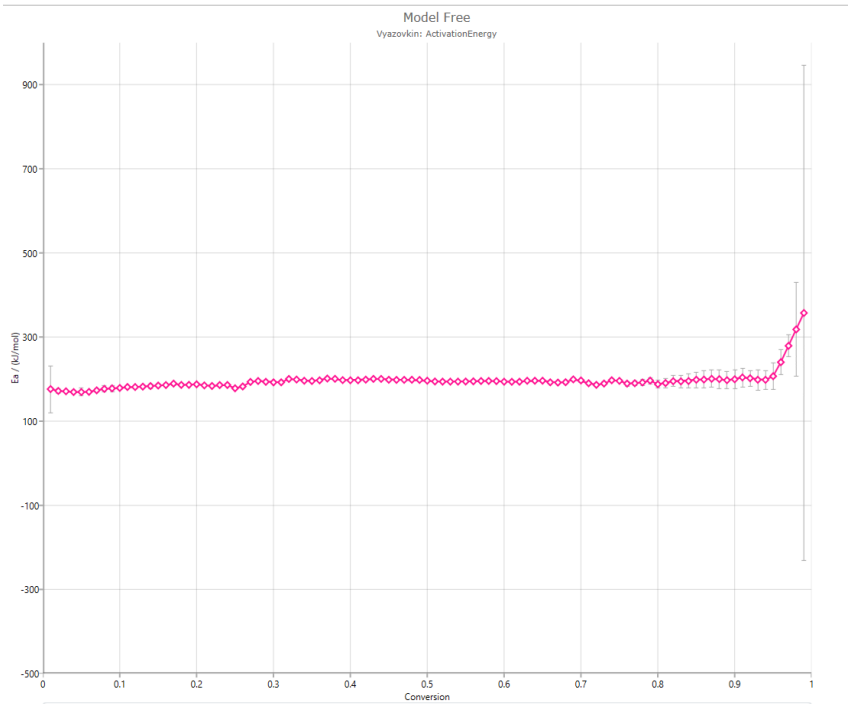

Figure 4.1: PET Batting E_a vs α plot (Isoconversional method)

The second method is the model-based analysis, which is based on the differential form of the basic rate equation (4.2) and is represented as:

$$\frac{d\alpha}{dT} = \frac{A}{\beta} \cdot exp\left[-\frac{E_a}{RT}\right] \cdot f(\alpha) \quad (4.3)$$

This is the non-isothermal rate law where $\frac{d\alpha}{dT}$ is the conversion with respect to temperature and β is the heating rate in K min^{-1}. This makes the reactions a temperature dependent process which can be tracked through the STA analyses. In the model-based method, the pyrolysis process is considered as a sum of signals of individual reactions which are individually described by the function $f(\alpha)$. The kinetic parameters are assumed to be constant throughout the progress of the individual reaction which essentially provides the kinetic parameter values for the particular reaction. The software required at least two TGA normalized mass curves collected at different heating rates to predict the kinetic parameters. Three heating rate TGA curves for each material were obtained from the STA testing of the materials. The output files from the STA experiment formed a basis for input to the Kinetics NEO software. The parameter values were investigated by adding the three heating rate curves of each material and entering the hypothesized reaction mechanism from the analyzed DSC data. For each individual reaction an individual function $f(\alpha)$ was assigned from the list of available functions and the literature recommendations. Using the adjustment functions in the software, which adjusts the kinetic parameter values as well as allows changing the timeline of the occurrence of a reaction, the fit of individual reactions was improved and matched

to the experimental curve as close as possible. The fit of the Kinetics NEO generated curve compared to the experimental curve is presented in figure 4.2 which is for polyester batting. Similar curves were obtained for other materials as well. The built-in optimize function in the software then optimizes the values and the software tries to generate a fit to the normalized mass curves based on the kinetic parameter values. The fitting of the curve is judged using the statistical analysis R^2 term which is essentially providing the estimate of the goodness of fit of the model curve based on the kinetic parameters. The closer the value of R^2 to 1, suggests the better the fit, however since completely different values can also provide an R^2 value close to 1 since it is based on a statistical model, the initial fit is provided by the user. For the model-based methods three functions viz. first order, second order and n^{th} order, for the $f(\alpha)$ term were considered and verified for fit to the experimental data. The n^{th} order reaction type was deemed to be fitting best based on the R^2 value for all the material fits. Although the n^{th} order reaction has little physical significance, but it creates a simplified mathematical fit to the experimental data with minimum number of reactions that can satisfy the reaction mechanism. The R^2 values for all the material curve fittings are provided in table 4.5. The nth order reaction is given by:

$$f = e^n \tag{4.4}$$

The values of the kinetic triplets for each of the materials' individual reactions determined using the Kinetics NEO software are provided in table 4.11 to table 4.15. The reaction mechanism with mass fractions of components is presented

in table 4.6 to table 4.10. In the tables the subscript ‘a’ denotes virgin material and subscripts ‘b’, ‘c’, ‘d’…. denote the intermediate products in the reactions.

For PET batting and PET fabric, a separate melting reaction was not shown and rather the heat of reaction of the melting process was combined with the first degradation reaction. Additionally, it was assumed that the three polymers did not have enough moisture in them which was confirmed by the fact that after drying there was no difference in the weights of the dried samples vs the virgin samples. Only MDF and OSB were considered to have significant moisture in them which considerably reduced the weight of the samples after drying and a moisture evaporation reaction was modeled in the FDS cone model. The kinetic parameters for the reaction were considered from literature [35][36] to be $A = 6.14\ sec^{-1}$, E_a = 23.5 kJ/mol and heat of reaction = $2.45 \times 10^7\ J\ kg^{-1}$.

Table 4.5: R^2 values for TGA inverse curve fitting for all materials

Material	**R^2 Value**
PUF	0.99996
PET BAT	0.99997
PET FAB	0.99979
MDF	0.99977
OSB	0.99978

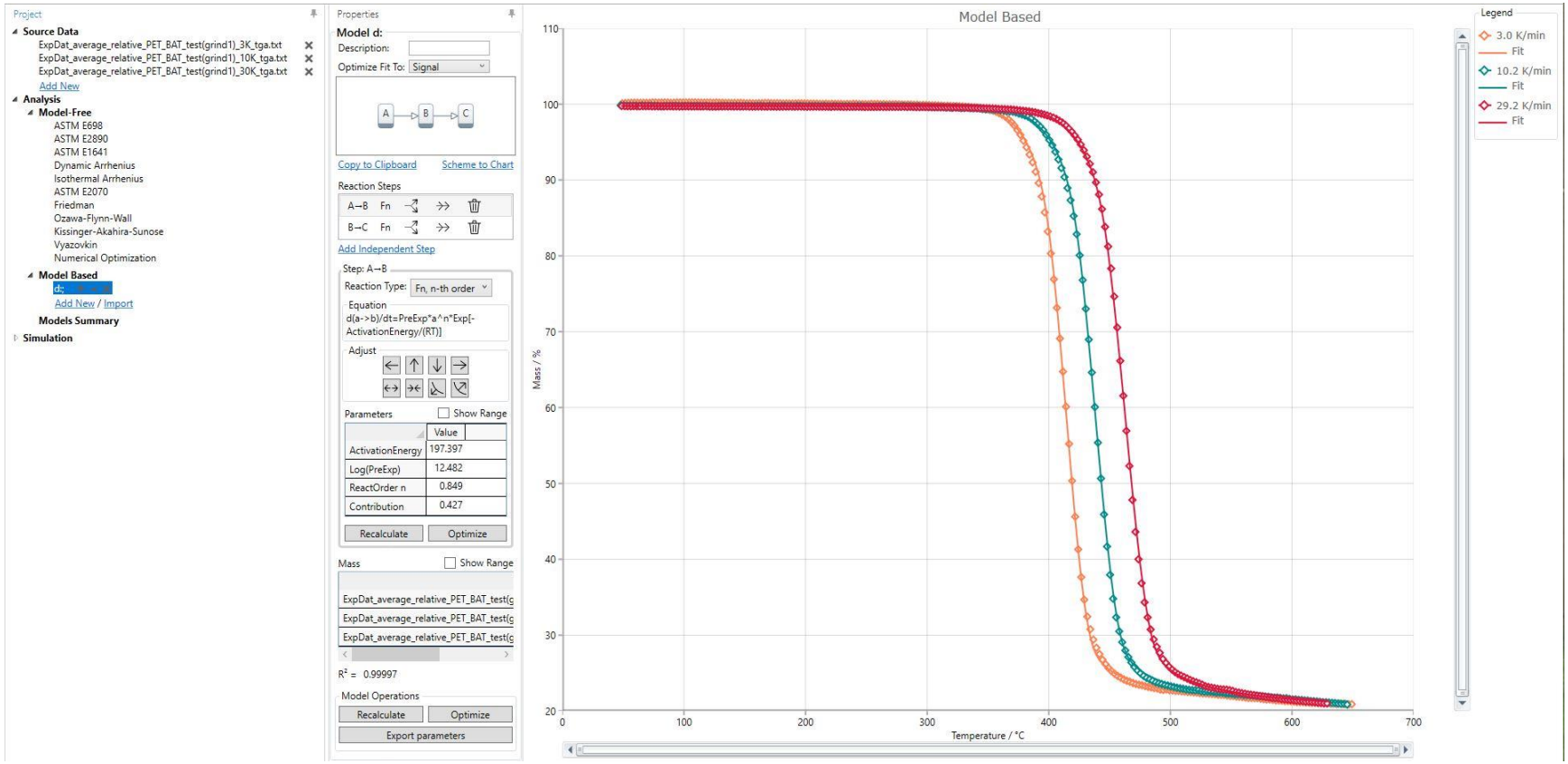

Figure 4.2: Kinetics Neo window for PET Batting

Table 4.6: Pyrolysis Reaction Mechanism for PU foam

Reaction #	Reaction Equation
1	$PUF_a \longrightarrow 0.74\ PUF_b + 0.26\ PUF\_gas2$
2	$PUF_b \longrightarrow 0.58\ PUF_c + 0.42\ PUF\_gas2$
3	$PUF_c \longrightarrow 0.06\ Residue + 0.94\ PUF\_gas3$

Table 4.7: Pyrolysis Reaction Mechanism for Polyester Batting

Reaction #	Reaction Equation
1	$PET\_BAT_a \longrightarrow 0.66\ PET\_BAT_b + 0.34\ PET\_BAT\_gas1$
2	$PET\_BAT_b \longrightarrow 0.32\ Char + 0.68\ PET\_BAT\_gas2$

Table 4.8: Pyrolysis Reaction Mechanism for Polyester Fabric

Reaction #	Reaction Equation
1	$PET\_FAB_a \longrightarrow 0.87\ PET\_FAB_b + 0.13\ PET\_FAB\_gas1$
2	$PET\_FAB_b \longrightarrow 0.29\ PET\_FAB_c + 0.71\ PET\_FAB\_gas2$
3	$PET\_FAB_c \longrightarrow 0.68\ Char + 0.32\ PET\_FAB\_gas3$

Table 4.9: Pyrolysis Reaction Mechanism for Medium Density Fiberboard

Reaction #	Reaction Equation
1	$MDF_a \longrightarrow 0.95\ MDF_b + 0.05\ MDF\_gas1$
2	$MDF_b \longrightarrow 0.74\ MDF_c + 0.26\ MDF\_gas2$
3	$MDF_c \longrightarrow 0.66\ MDF_d + 0.34\ MDF\_gas3$
4	$MDF_d \longrightarrow 0.41\ Char + 0.59\ MDF\_gas4$

Table 4.10: Pyrolysis Reaction Mechanism for Oriented Strand Board

Reaction #	Reaction Equation
1	$OSB_a \longrightarrow 0.76\ OSB_b + 0.24\ OSB\_gas1$
2	$OSB_b \longrightarrow 0.5\ OSB_c + 0.5\ OSB\_gas2$
3	$OSB_c \longrightarrow 0.51\ Char + 0.49\ OSB\_gas3$

Table 4.11: Reaction Kinetic Parameters for PU Foam

Reaction #	A (sec^{-1})	E_a (kJ/mol)	n	contribution	h (J kg^{-1})
1	9.225×10^{11}	152.536	0.965	0.264	2.65×10^6
2	5.105×10^{12}	183.983	0.514	0.324	1.44×10^6
3	1.655×10^{14}	201.095	1.648	0.412	2.87×10^6

Table 4.12: Reaction Kinetic Parameters for Polyester Batting

Reaction #	A (sec^{-1})	E_a (kJ/mol)	n	contribution	h (J kg^{-1})
1	3.03×10^{12}	197.397	0.849	0.427	1.7×10^6
2	7.64×10^{13}	194.034	3.741	0.573	4.81×10^6

Table 4.13: Reaction Kinetic Parameters for Polyester Fabric

Reaction #	A (sec^{-1})	E_a (kJ/mol)	n	contribution	h (J kg^{-1})
1	1.435×10^4	83.838	0.679	0.153	0.8×10^6
2	1.458×10^{19}	286.844	1.094	0.749	3.6×10^6
3	5.675×10^9	166.775	3.488	0.098	1.8×10^6

Table 4.14 Reaction Kinetic Parameters for Medium Density Fiberboard

Reaction #	A (sec^{-1})	E_a (kJ/mol)	n	contribution	h ($J\ kg^{-1}$)
1	1.028×10^{16}	170.780	2.943	0.064	0.23×10^{6}
2	4.808×10^{9}	130.809	1.296	0.306	0.45×10^{6}
3	3.689×10^{15}	204.992	1.826	0.295	0.91×10^{6}
4	7.888×10^{15}	179.927	9.983	0.335	-0.56×10^{6}

Table 4.15 Reaction Kinetic Parameters for Oriented Strand Board

Reaction #	A (sec^{-1})	E_a (kJ/mol)	n	contribution	h ($J\ kg^{-1}$)
1	1.55×10^{10}	129.793	2.794	0.293	0.48×10^{6}
2	2.37×10^{13}	179.614	1.55	0.478	1.31×10^{6}
3	1.3×10^{17}	211.485	10.522	0.229	-1.43×10^{6}

4.2.6 Heat of combustion:

The heat of combustion for the fuels in the material was determined using the MCC data. The FDS model for TGA analysis was populated with the kinetic parameters, other measured data and the entered heat of combustion value based on the maximum value of heat released from the MCC data. The model generated an MCC curve whose total area was not equal to the MCC data which was expected (figure 4.3 left). Further analysis was conducted, and a heat of combustion value was fit manually to match the peak HRR of the MCC curve (figure 4.3 right). There was a slight mismatch between the two curves and the FDS model curve shifted towards the right by 12 K. This discrepancy was attributed to the fact the crucible is open top and the temperature at the top surface - being additionally heated by radiation from the combustor - was not fully captured by the MCC sample temperature sensor located below the sample crucible. The fit of the FDS curve was very close to the MCC curve and hence the value of the heat of combustion was considered for all reactions.

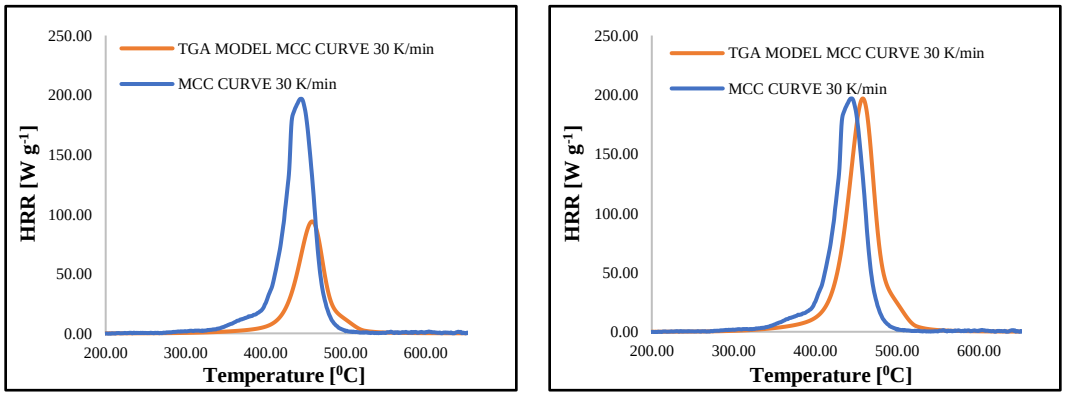

Figure 4.3: TGA model curve vs MCC curve initially (left image) and TGA model curve vs MCC curve after peak heat release rate matching (right image)

4.2.7 Heat of reaction:

The heat of reaction considered for the fuels that are present in the tested materials was determined using the DSC data. As per the reaction mechanism outlined in section 4.2.5 and the contribution of each reaction determined from the kinetic analysis procedure detailed in section 4.2.5, the DSC curve was analyzed against the normalized mass curve of the TGA to identify the start and end of the reaction. The heat of reactions was then obtained by integrating the area under the DSC curve for the individual reactions. The heat of reactions for all materials and their individual reactions are as mentioned in table 4.11 to table 4.15. The DSC curves were not repeatable between heating rates and within heating rates due to a baseline issue with the instrument. Hence the individual heating rates were observed and the heating rates with most repeatable DSC curves were considered and the values of heat of reaction found for all the reactions which were considered in the FDS model.

4.3 Milligram-scale modeling

The FDS condensed phase solver provides a platform to develop complex pyrolysis models by considering the reaction mechanism and kinetics that takes place during the pyrolysis of the material. The model was developed using the FDS User Guide [47] and the important inputs are detailed in this section. The simulation in the FDS for these experiments is with a consideration of thermally thin conditions with a 0D model. The FDS code mimics the TGA, DSC and MCC outputs by addition of a flag TGA_ANALYSIS=.TRUE. and heating rate condition

input using TGA_HEATING_RATE. These two lines added in the code forces FDS to perform a numerical version of the three tests and all other boundary conditions are ignored. The analysis is very short and the FDS codes shuts down without running an actual simulation and provides the results for the three measurements.

4.4 Cone calorimeter modeling

Cone model was developed using the FDS User Guide [47] to simulate the cone in a 1-D condensed phase model using the data generated from the various measurement techniques outlined in section 4.2. Additional, guidelines have been elaborated in this section to develop the model suitable for the application in this study. A grid with minimum cells was essentially modeled for the pressure solver to work effectively. Since the materials in this study are non-standard and are not in the FDS library, they were defined using the REAC line with a basic fuel that the material was made of. The produced species that was defined to be generated after the pyrolysis of the material was considered to be of the same fuel that was defined in the REAC line and heat of combustion considered for the gas was same as the heat of combustion of the fuel that was determined as outlined in section 4.2.6. The top surface of the material is modeled as a plane in FDS on which an external heat flux was imposed. The back surface of the cone model in FDS is insulated in which case no heat is lost to the backing material.

Additionally, since the gas phase modelling was not used in the simulation of the cone model, flame heat feedback was modelled in the cone calorimeter model as per the recommendations made in the prior study conducted by McCoy & Tilles

[37]. They conducted cone calorimeter tests on various polymers to develop a generalized flame model. They measured the heat fluxes incident on the material surface using water cooled Schmidt-Boelter gauges at two locations, center and sides of the sample. This study provided a flame heat feedback model based on the convective and radiative heat feedback at the center and the edge of the sample. Their model of flame heat feedback is presented in table 4.16.

Table 4.16 Flame Heat Feedback Model (McCoy & Tilles)

Heat Flux	Center Zone (54mm square)		Side Zone (outside center zone)	
	Pre - ignition	Post ignition	Pre - ignition	Post ignition
Convective ($kW\ m^{-2}$)	9×10^{-3} (T_s - 300)	3.7×10^{-3} (2150-T_s)	12.7×10^{-3} (T_s-300)	20×10^{-3} (2150-T_s)
Radiative ($kW\ m^{-2}$)	q''_{cone}	$q''_{cone} + 9.5$	$0.95\ q''_{cone}$	$0.95\ q''_{cone}$

To model this in FDS, four FDS files were developed for each material for each case presented in table 4.16. The reaction mechanism was kept same in all the four files. The pre-ignition files had a stop functionality which would run up to a particular time and then stop. This was accomplished using the RESTART convention in the FDS model. The pre-ignition files were stopped at the ignition time which was considered from the cone test data. The post ignition files started

calculating data from the point where the pre-ignition files stopped. Through this process we obtained two HRR .csv files as output that had the MLRPUA for each case. In each of the file the radiation flux was defined through EXTERNAL_FLUX line. The convective radiation was defined using the two lines of code where ASSUMED_GAS_TEMPERATURE line was used on which the assumed surrounding gas temperatures were defined, and the heat transfer coefficient was defined using the HEAT_TRANSFER_COEEFICIENT line and the values entered were considered as per table 4.16. FDS calculates the T_S (surface temperature) on its own and considers the application of the convective heat flux application using the convective heat flux equation given as:

$$\dot{q}_c'' = h\left(T_g - T_w\right) \tag{4.5}$$

Where, $\dot{q}_c''$ (W m^{-2}) is the convective heat flux to the surface, h (W m^{-2} K^{-1}) is the heat transfer coefficient, T_g (^{0}C) is the surrounding gas temperature which is user defined and T_w (^{0}C) is the wall (surface) temperature which is calculated by FDS. The equation is similar to the ones given in table 4.16.

The gas phase grid resolution is not important in the condensed phase modeling given FDS solves the one-dimensional heat transfer equation numerically [47], though it does use the node spacing for the numerical solution. Due to this the solid phase numerical grid becomes an important point to focus upon in the model. For condensed phase, the stability and numerical accuracy of the solution depends on four parameters. First is making the node spacing perfectly uniform which was

done in the study by using the command line STRETCH_FACTOR = 1. The mesh size was kept default at 1 and can be changed by using the command CELL_SIZE_FACTOR='value', where the value input can be used to set the values of the cell size below 1. The next parameter was the time resolution which was controlled by using WALL_INCREMENT=1 on the TIME line and sets up to update the solid phase solution every time step. Finally, the number of cells in each layer can be changed by using N_LAYER_MAX (:) to set the value using the array. For this study the default value of 1000 was used, and the value can be reduced for models which have a lot of reactions thereby reducing the time of computation though it does not affect much the accuracy of the solution.

Chapter 5: Computational Modeling Results and Discussion

5.1 Milligram-scale model

The 0-D model developed for the milligram scale predictions was populated using the properties determined in section 4 and the model predictions for 30 K min^{-1} were compared and plotted against the experimental data at the same heating from the STA. The plots for all five materials are shown in figures 5.1 to 5.5 below. The FDS model predictions overall provide a good match to the experimental data. The position and shape of the TGA and the MLR curve are a good match as well as the peaks of the MLR curves are the same as that of the experimental curve within the uncertainties of the model. The final residue yield for the materials is accurately predicted by the model and match the residue obtained in the TGA experiments.

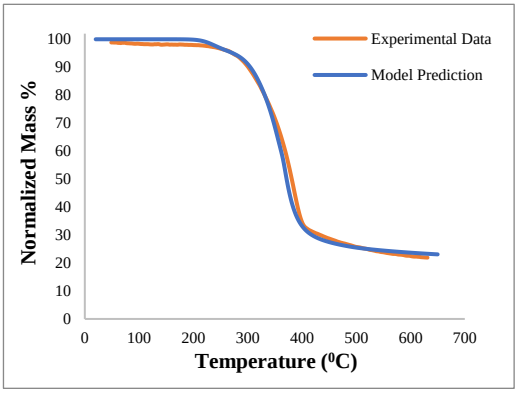

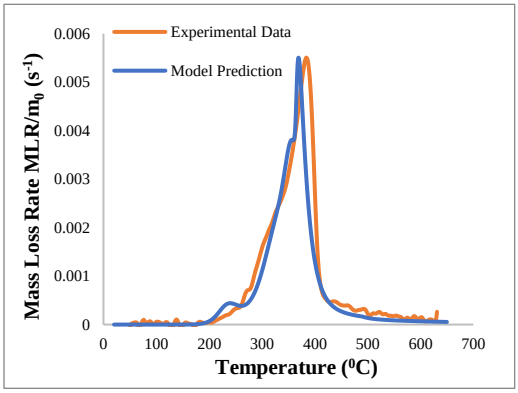

Figure 5.1: Medium Density Fiberboard Normalized mass curve and Mass Loss rate curve for 30 K/min heating rate

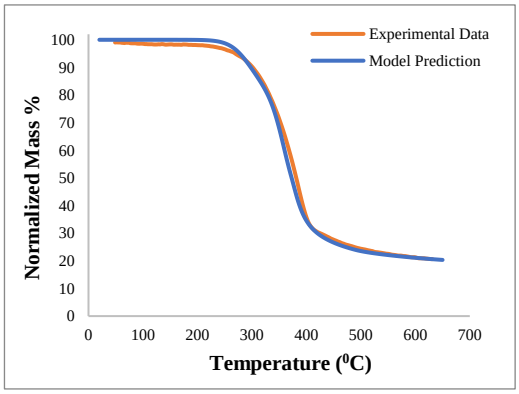

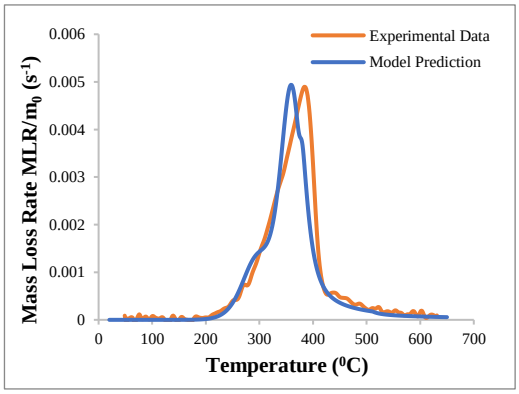

Figure 5.2 Oriented Strand Board Normalized mass curve and Mass Loss rate curve for 30 K/min heating rate

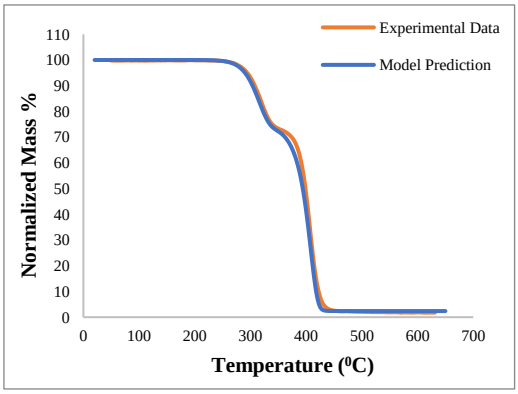

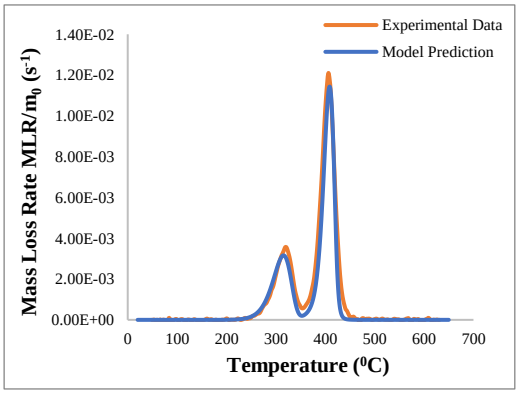

Figure 5.3 Polyurethane foam Normalized mass curve and Mass Loss rate curve for 30 K/min heating rate.

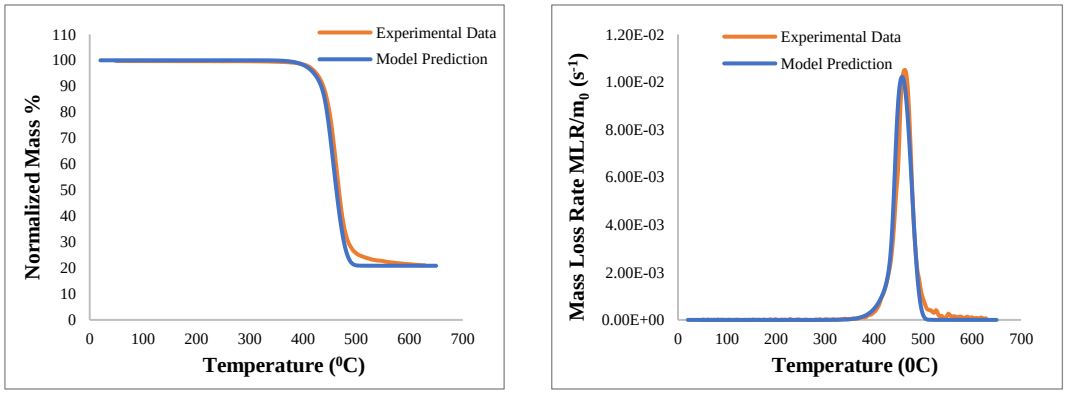

Figure 5.4 Polyester Batting Normalized mass curve and Mass Loss rate curve for 30 K/min heating rate

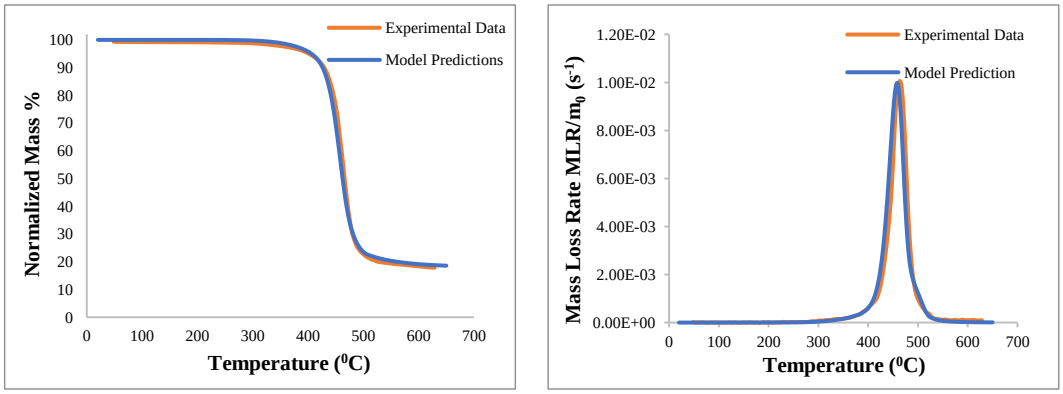

Figure 5.5 Polyester Fabric Normalized mass curve and Mass Loss rate curve for 30 K/min heating rate

5.2 Cone model

Forty-five cone calorimeter tests were performed for the five materials to obtain the experimental data for model validation. Three tests each were conducted at 25 kW m^{-2}, 50 kW m^{-2} and 75 kW m^{-2} heat fluxes for each of the 5 materials. In the FDS model the area of the sample was considered as 1 m^{-2} so the mass loss rate (MLR) generated is independent of the area of the sample and provides a normalized mass loss rate (MLR) curve or mass loss rate per unit area (MLRPUA) for each of the materials at each of the heating rates.

In FDS to apply the flame heat feedback model with pre-ignition and post ignition applicability, RESTART functionality was used. The cone calorimeter samples are 100 mm x 100 mm in area and the flame heat feedback model was divided into two zones, one a center zone of 54 mm square and the other side zone with rest of the area. In total 4 FDS files for each material were created for pre-ignition & post ignition for each of the two zones. This generated two .csv files for two zones which provided the MLRPUA. The contribution of MLRPUA from each of the two zones was calculated using an area fraction $\frac{A_{zone}}{A_{Total}}$ which came out to be 0.3 for center zone and 0.7 for the side zone. So, the total MLRPUA was found using:

$$MLRPUA = 0.3 * MLRPUA_{center} + 0.7 * MLRPUA_{side}$$

The heat of combustion that was found using the FDS TGA model and MCC tests was used for creating area normalized Heat release rate or Heat release rate per unit area (HRRPUA) curves from the MLR output using the following formula:

$$\dot{Q}''(kW\ m^{-2}) = \dot{m}''(kg\ s^{-1}\ m^{-2}) \cdot \Delta h_c\ (kJ\ kg^{-1})$$

Where, $\dot{Q}''$ is the HRRPUA, $\dot{m}''$ is the MLRPUA from the FDS model and Δh_c is the heat of combustion.

The curves generated using the above equation were plotted against the cone calorimeter outputs to compare and validate the model outputs. Figure 5.6 to 5.19 present the plotted comparison graphs for all the materials at each of the heat fluxes and features and differences for each material are discussed. The figures show the HRRPUA curves from three different tests and an average HRRPUA curve compared against the FDS model generated results.

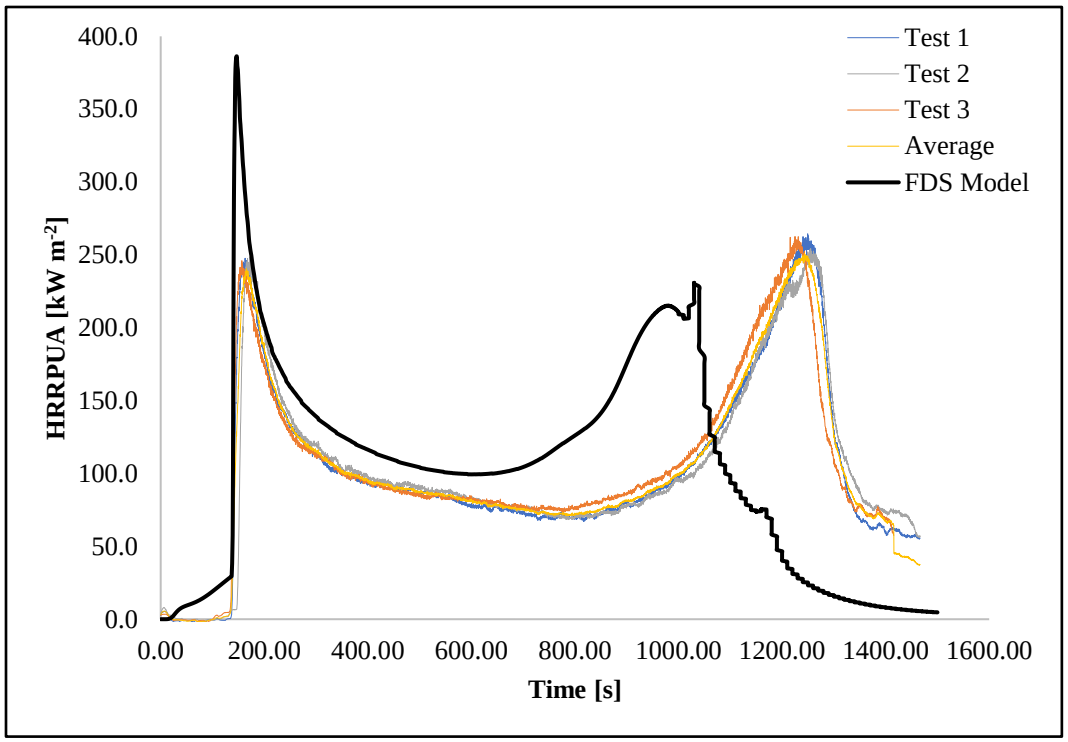

Figure 5.6: HRRPUA for MDF 25 kW m^{-2}

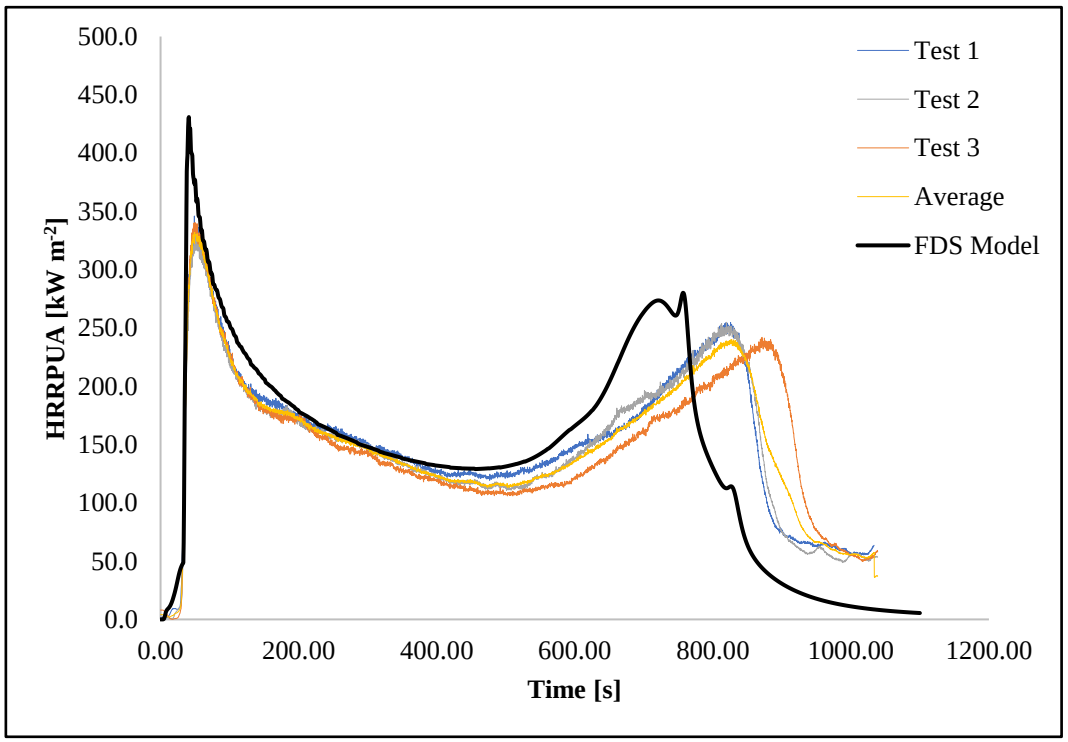

Figure 5.7: HRRPUA for MDF 50 kW m^{-2}

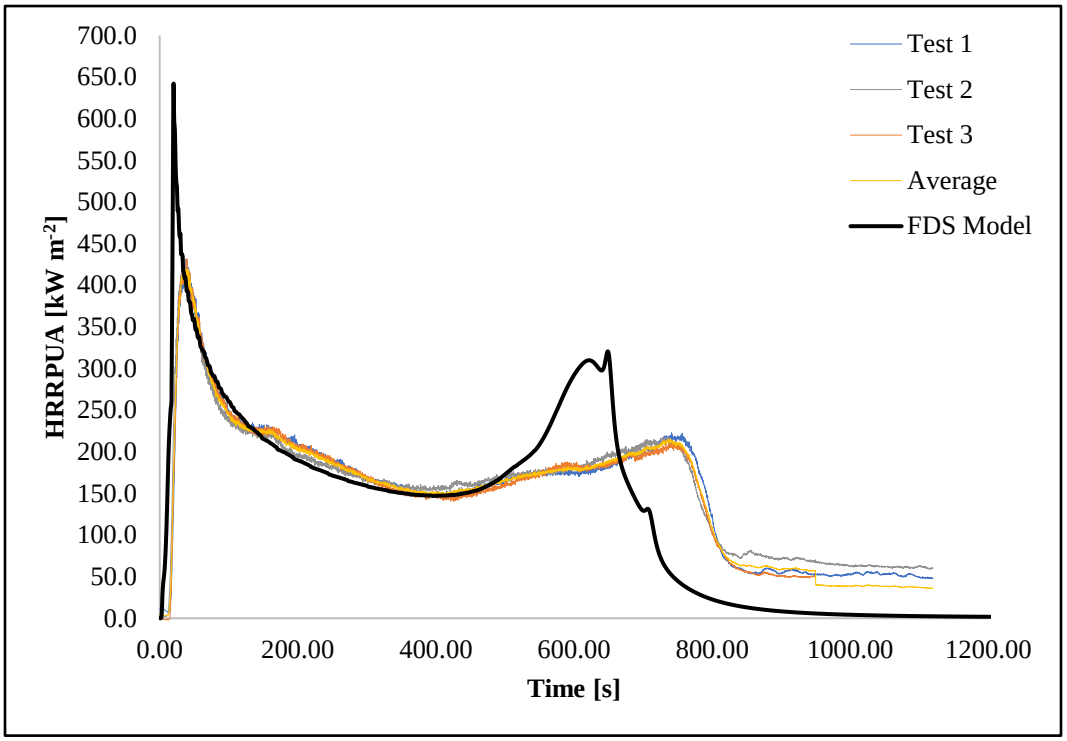

Figure 5.8: HRRPUA for MDF 75 kW m^{-2}

For MDF the model captures the peak location of the first peak correctly but significantly overestimated the magnitude of the peak in the 25 kW m^{-2} plot by about 56% (140 kW m^{-2}). The model also overpredicted the first peak magnitude in the 50 kW m^{-2} and 75 kW m^{-2} but the percentage overprediction (26% and 45% respectively) was lower at larger heat fluxes. Additionally, the model conformed well with the cone test data after the first peak and then predicted the second peak early in time for all the three heating rates, however the magnitude of the second peak was well captured by the model for 25 kW m^{-2} and 50 kW m^{-2} while over predicting for 75 kW m^{-2} by about 50%. The differences in the model predictions and the cone data were a cumulative effect that can be attributed to the fact that the temperature dependent properties of thermal conductivity and specific heats are

important in the model development which in our case was extrapolated from the values at room temperatures. Additionally, the DSC curves were not repeatable due to a problem in the baseline of the DSC instruments at the lab. This resulted in varying values of heat of reactions across heating rates. The heat of reactions was thus considered from the heating rate curve which provided some repeatability in the generated curves than the other heating rates. Another reason for the first peak's increase magnitude is the constant heat of combustion consideration for all the reactions. The method described in section 4.2.6 did provide a good approximation of the global heat of combustion, but the peak can be improved by determining a separate and varying heat of combustion for different reactions.

There are quite a few parameters that need to be further investigated out of which the aspects of temperature dependent properties are straightforward measurements using the apparatus. Additionally, reproducibility of the signals from the DSC can be improved improving the baseline in the instrument which will result in better judgement for heats of reactions. Further since the flame heat feedback model provides application of same empirical model to all heat fluxes, it may be providing elevated magnitudes of the HRRPUA values at lower heat fluxes which can be further investigated to improve the model for lower heat fluxes.

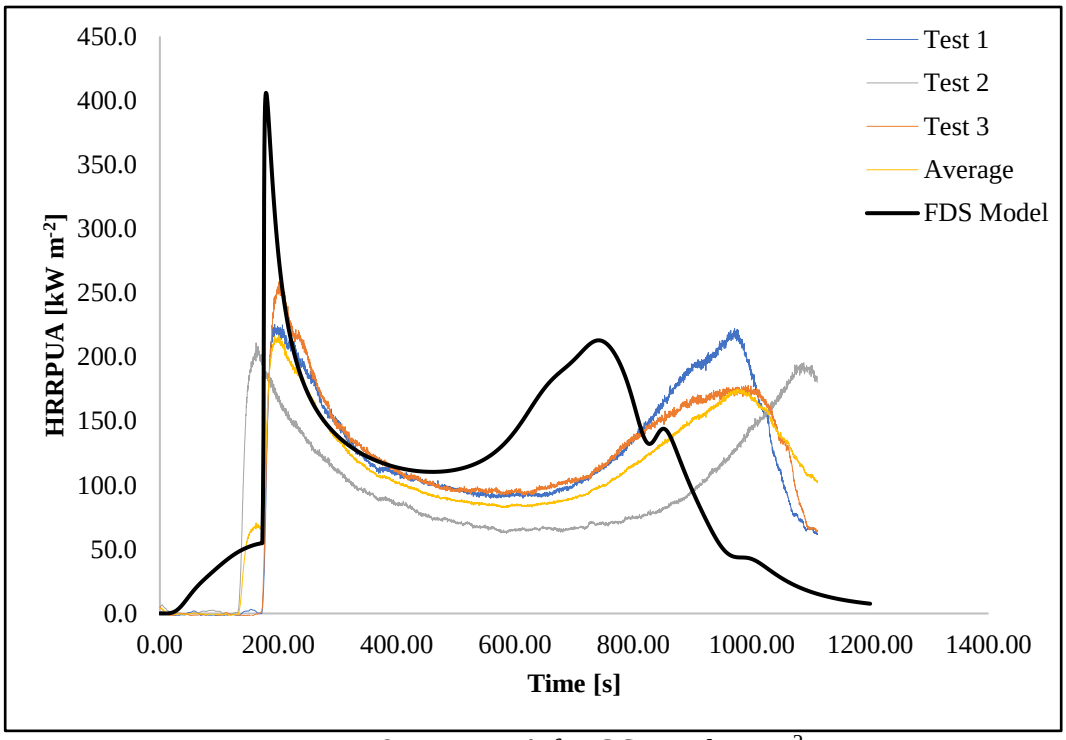

Figure 5.9: HRRPUA for OSB 25 kW m^{-2}

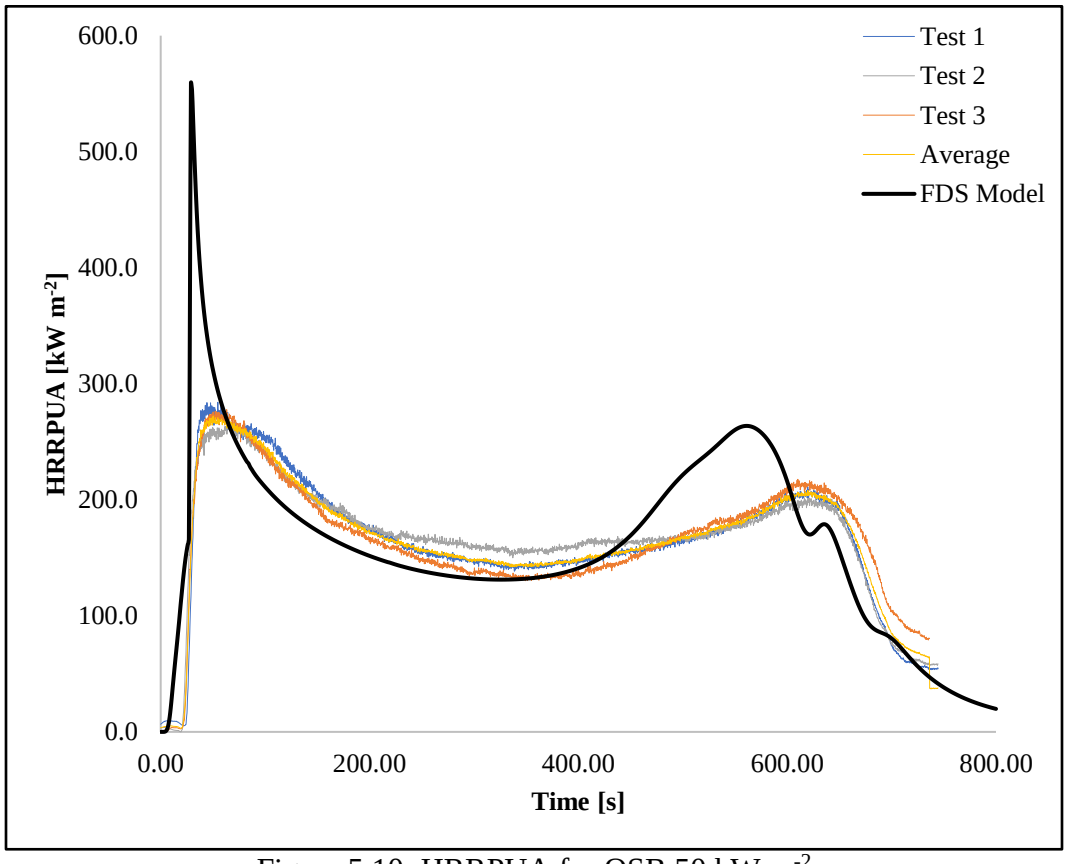

Figure 5.10: HRRPUA for OSB 50 kW m^{-2}

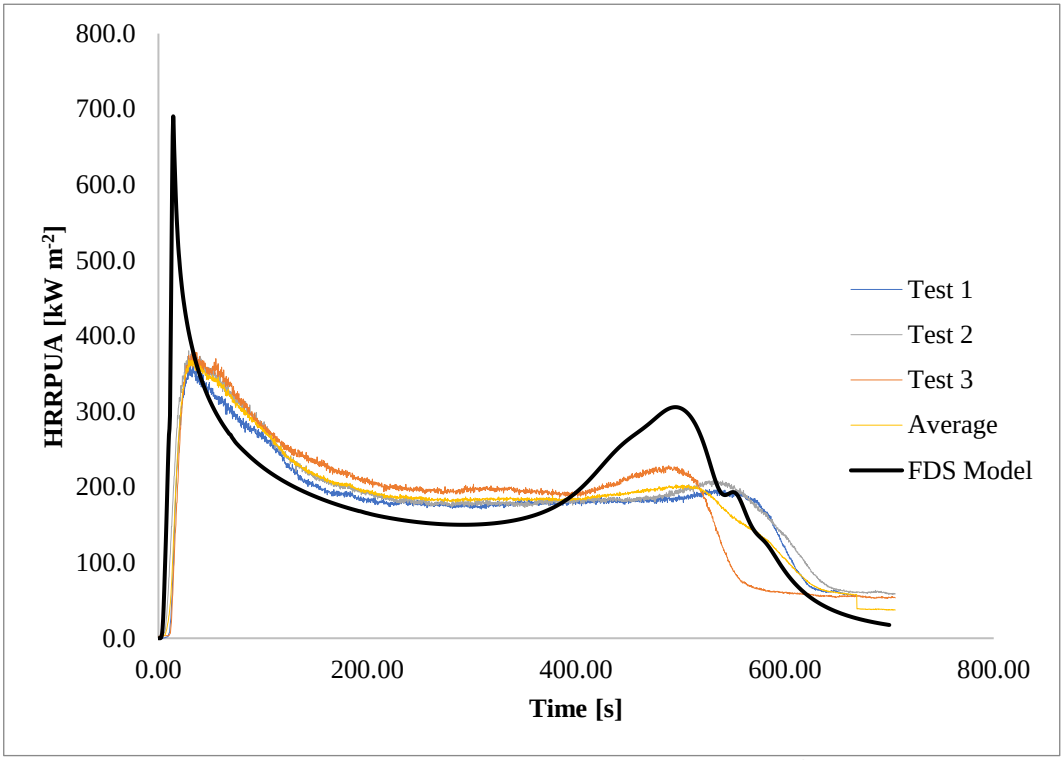

Figure 5.11: HRRPUA for OSB 75 kW m^{-2}

For OSB similar results to MDF were obtained from the FDS model where it captured the peak location of the first peak correctly but significantly overestimated the magnitude of the peak for all the heat fluxes (close to 100% for 25 kW m^{-2} and about 75% for 50 kW m^{-2} and 75 kW m^{-2}). Additionally, the model conformed well with the cone test data after the first peak and then predicted the second peak reasonably well for larger heating rates, however the magnitude of the second peak was captured was similar to MDF (better agreement to lower heat fluxes and not so 50% over for 75 kW m^{-2}). Similar to MDF the differences in the model predictions and the cone data were a cumulative effect of non-availability of the temperature dependent properties of thermal conductivity and specific heats as well as DSC curves not being repeatable. The first peak's increase magnitude here can also be attributed to the constant heat of combustion consideration for all the reactions and

can be improved by having a separate and varying heat of combustion for different reactions. For the OSB model as well the improvements in reproducibility of the signals from the DSC as well as determination of temperature dependent thermal properties will improve the model considerably. Finally, the flame heat feedback model can be further investigated to improve the model for lower heat fluxes.

The observation of second peak in both wood based products is attributed to the fact that the material is thermally thick, the heat travels slowly through the solid and heats & pyrolyzes the inner layers and is concentrated there as the back surface is insulated. As soon as the top layers of the solid combust they leave behind porous char layers, which lets the inner heated and pyrolyzed products to come up to the surface and participate in the combustion process thus creating a spike towards the end. The FDS model developed with BACKING = INSULATED command did capture this phenomenon well, resulting in the later spike in output.

For MDF (25 kW m^{-2}) & OSB (25 kW m^{-2}), the duration of combustion was significantly lower (about 250 seconds each) for the FDS model predictions compared to the actual tests. This is attributed to the fact that there is a cumulative effect of the factors discussed above but the biggest contributing factor is the flame heat feedback model. The study by McCoy & Tilles [37] provided the flame heat feedback model by considering the average of 8 different thermoplastic materials. Additionally, the results from their study did provide burn times that were on the higher side by about 200 secs as compared to the actual tests, for materials like poly(oxymethylene) (POM) at smaller heat fluxes of 20.6 kW m^{-2}. In this study for

higher heat fluxes the values of burn time from FDS model were close to the experimental results for the larger heat fluxes of 50 & 75 kW m^{-2}, for both wood based products. While OSB FDS predictions matched the experimental combustion duration, MDF FDS predictions were about 100 seconds off from the experimental data which can be attributed to the absence of heat of reactions from the repeatable DSC tests.

For the three polymers considered in this study, the FDS model did not provide a good output when compared to the cone tests. For the PU foam the model did provide a decent fit for the initial 40-50 seconds for the 25 kW m^{-2} heat flux. For larger heat fluxes albeit the magnitude of HRRPUA being off the model did predict the general trend initially but after the initial burning the trend was not captured properly at all. The magnitude of HRRPUA being high can be attributed to larger heat of combustion consideration. The trend does not match after the initial seconds as PU foam when heated has a tendency to produce decomposition products that are in a liquid phase [44] when it combusts. It does not necessarily change phase itself but once it decomposes into liquid fuel products the properties of PU foam no longer apply to the phase changed product. Since liquids have greater densities than their virgin material as well as different material properties of thermal conductivity and specific heat than solidified material this has an effect on the model predictions. This can be improved by measuring properties of the phase change and applied to the model to get better predictions.

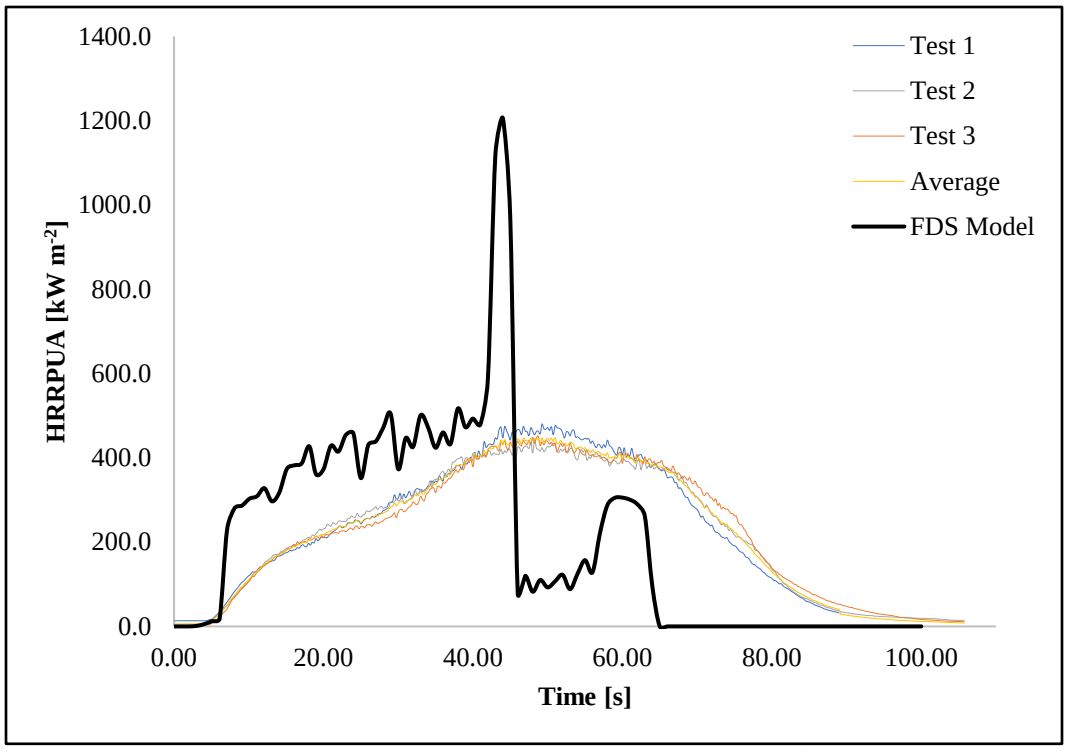

Figure 5.12: HRRPUA for PUF 25 kW m^{-2}

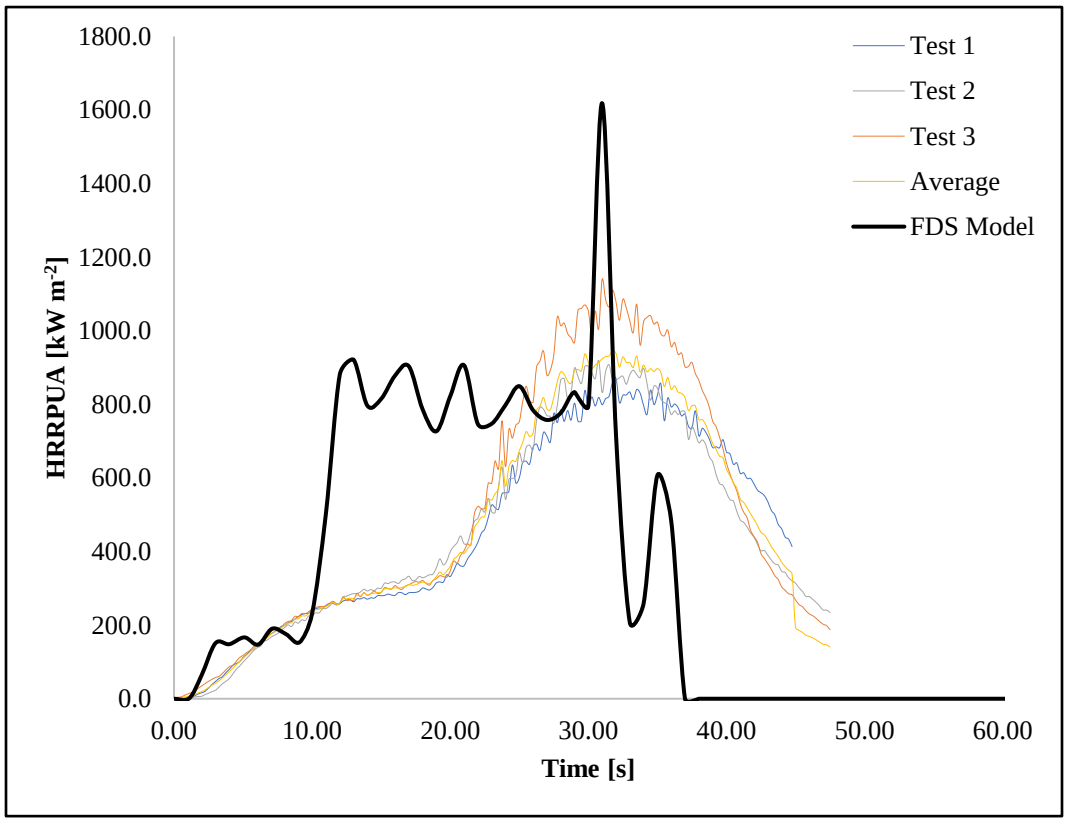

Figure 5.13: HRRPUA for PUF 50 kW m^{-2}

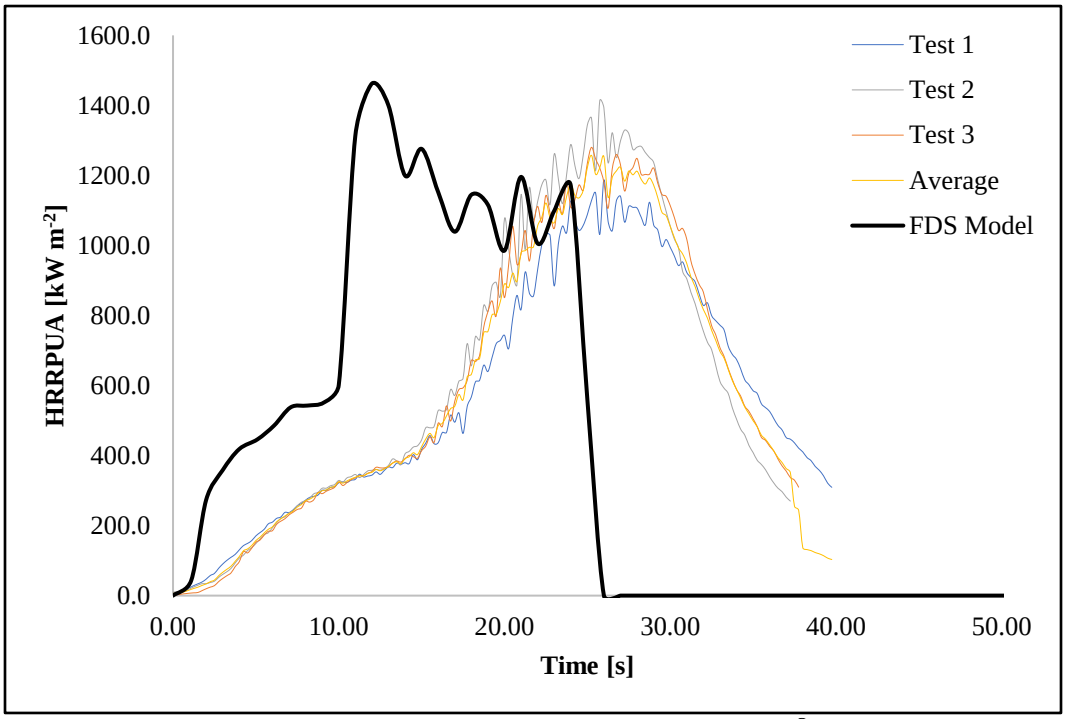

Figure 5.14: HRRPUA for PUF 75 kW m^{-2}

Similar to PU foam observations the model for polyester batting and polyester fabric do not provide a good fit to the experimental data. The polyester batting being a low density material has very low thermal inertia due to which the heat is concentrated on the surface and the temperature increases causing it to pyrolyze faster. In the condensed phase solver of FDS there is no apparent ignition that occurs, the MLR begins as soon as the computation starts. Additionally, the flame heat feedback model that was applied for pre ignition has a larger heat transfer coefficient which result in an increased convective heat flux on the surface of the material thereby increased MLR which can be seen in the larger heat flux plots where the HRRPUA is very high for the initial time and as soon as the post-ignition limit applies the curve begins to capture the general trend of the cone test.

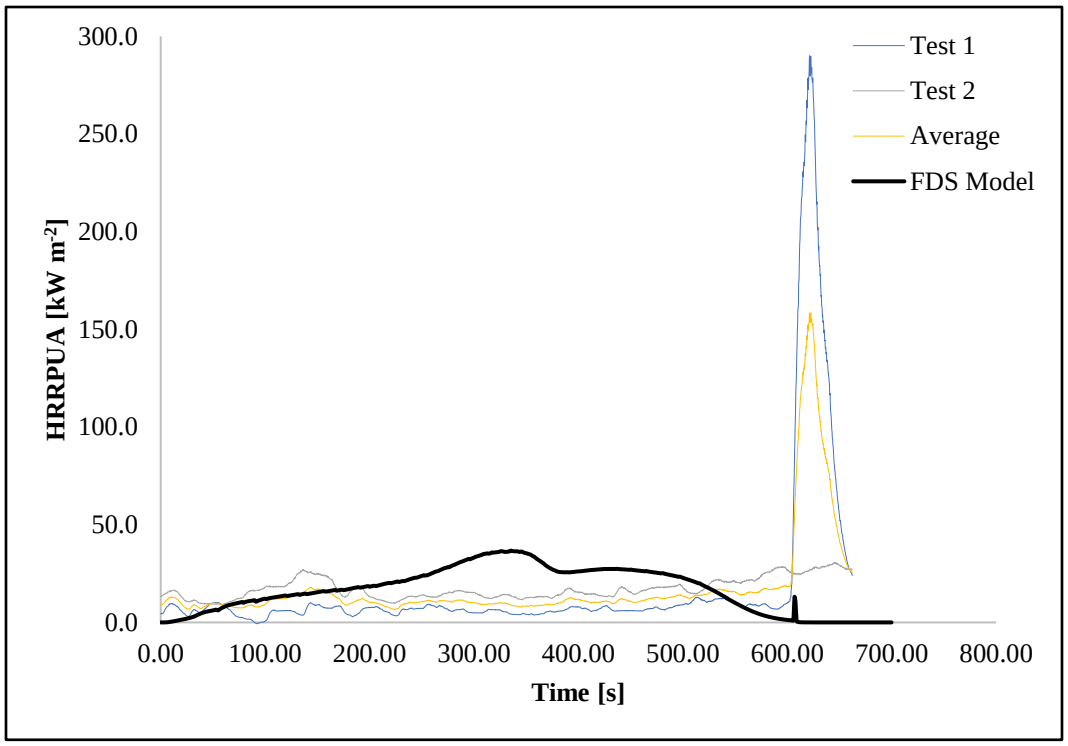

Figure 5.15: HRRPUA for PET BAT 25 kW m^{-2}

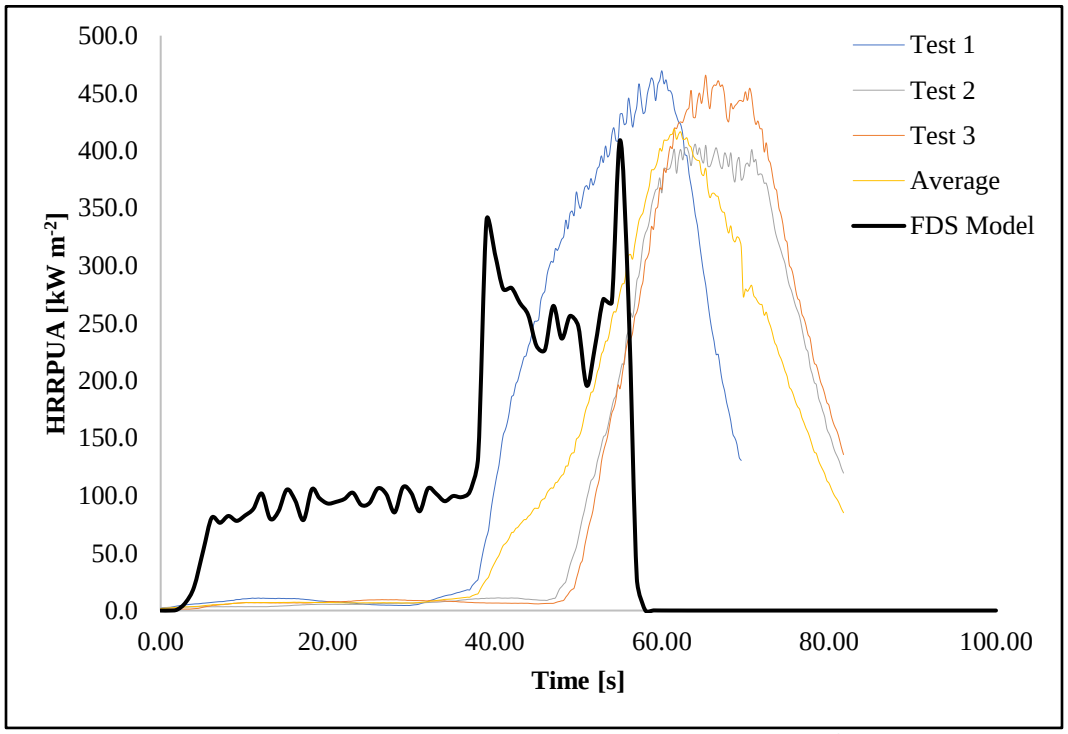

Figure 5.16: HRRPUA for PET BAT 50 kW m^{-2}

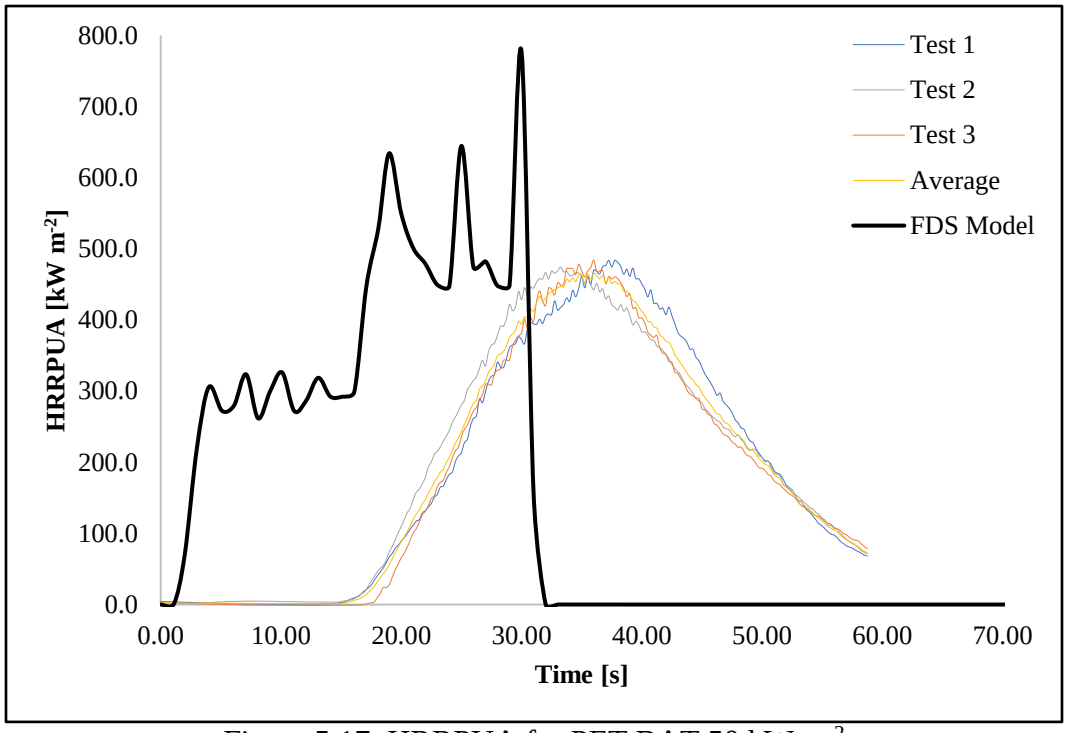

Figure 5.17: HRRPUA for PET BAT 50 kW m^{-2}

For polyester fabric similar to polyester batting, the thermally thick consideration for thermally thin materials does not qualify. The thickness of the polyester fabric tested under this study was 0.47 mm. This material can be defined as a thermally thin solid based on the simple criterion of Biot number (Bi) which should be less than 1 and which is given by the equation:

$$B_i = \frac{hL}{k}$$

Where h (W m^{-2} K^{-1}) is the global heat transfer coefficient, k (W m^{-1} K^{-1}) is the thermal conductivity and L (m) is the thickness of the material [SFPE handbook]. Given the low thickness of 0.00047 m of the fabric, the thermal conductivity at ambient of 0.03 W m^{-1} K^{-1} and the heat transfer coefficient defined

by the flame heat feedback model 9- & 12 W m^{-2} K^{-1} gives a very low Biot number which is thermally thin. Due to this the temperature of the surface increases rapidly resulting in huge convective heat flux on the sample and subsequent large MLR which is evident from the graphs that have a massive peaks before the onset of sustained ignition. So, the flame heat feedback model does not tend to work properly for the low thermal inertia materials or for thermally thin materials and hence the applicability of the flame heat feedback model needs to be investigated further. In addition to that the temperature dependent thermal properties as well as the heat of combustion as discussed for prior materials needs to be determined for the model to verify if they have a cumulative effect along with the flame heat feedback model.

Additionally, it can be seen for the PU foam and PET batting that there are a lot of oscillations in the FDS model outputs, the likely cause of these oscillations is insufficient resolution. As discussed in section 4.4 of this study the accuracy and stability of the solution can be improved by using the four command prompts. Using the default values in the study is a likely cause for the oscillations which can be improved by reducing the size of the mesh with the command line CELL_SIZE_FACTOR. There needs to be a determination of the same by changing the value below the default value of 1 to find the threshold that provides numerical stability and subsequently reduced oscillations.

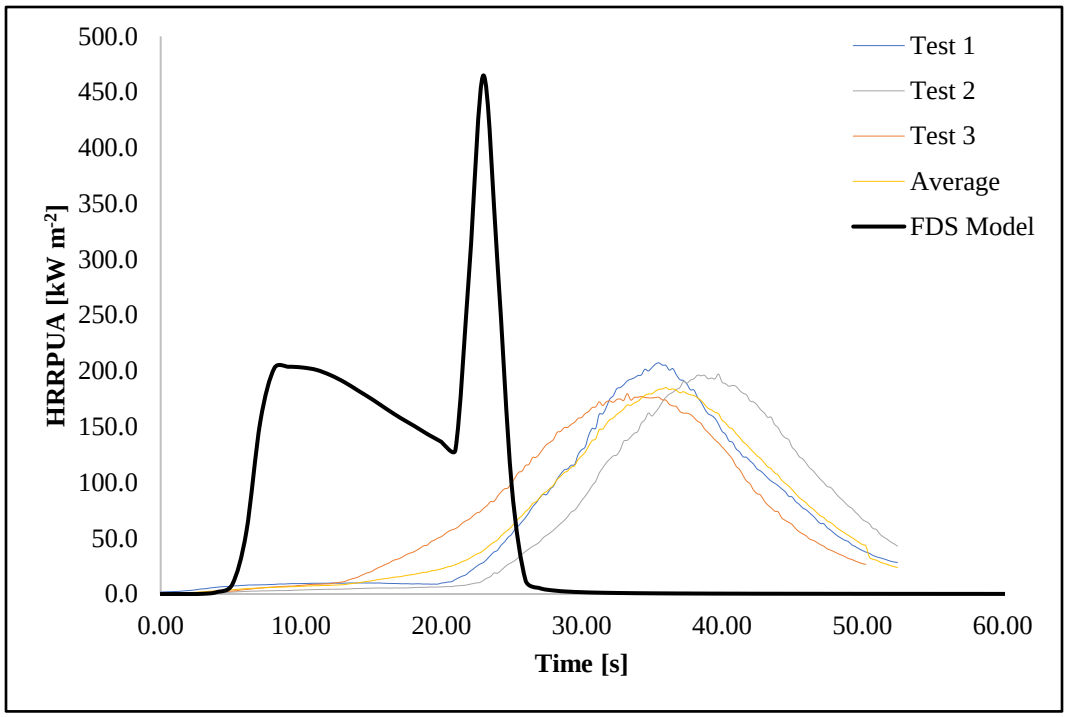

Figure 5.18: HRRPUA for PET FAB 50 kW m^{-2}

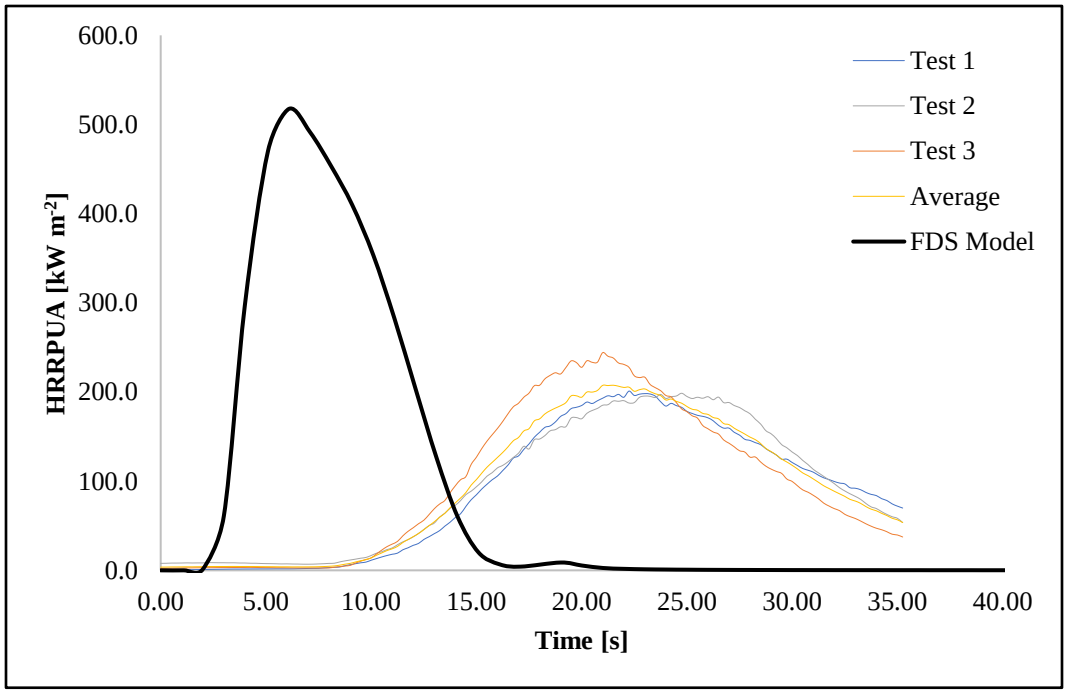

Figure 5.19: HRRPUA for PET FAB 75 kW m^{-2}

For the polymers in this study, the duration of combustion was lower for the FDS model predictions compared to the actual tests. The two major reasons are the density of the phase changed intermediates and the flame heat feedback model, with flame heat feedback model hypothesized to being the prime reason. The study by McCoy & Tilles [37], providing the flame heat feedback model was conducted on thermally thick and high thermal inertia polymers which provided long combustion durations of 300-800 seconds for larger to smaller heat fluxes. As compared to the polymers in this study which are low thermal inertia and thermally thin polymers, where the burn times range from 35-100 seconds (except for the polyester batting with 25 kW m^{-2} heat flux, which did not ignite until around the 600 second mark and was smoldering up until then). Additionally, PU foam and PET batting changes phase and melted which in actual test results in reduced heat flux at the top surface of the sample and subsequently longer combustion times in the actual test. The FDS models did provide a good general trend overall but the flame heat feedback resulted in higher HRR that meant a higher mass loss rate resulting in early consumption of the combustible material.

Chapter 6: Conclusions and Further work

In this study, material properties for five materials used in the built environment were measured. Milligram scale tests and other tests were performed using which the properties were quantitatively measured. Pyrolysis mechanism for all the five materials using the TGA signals were developed out of which Polyurethane Foam (PUF), Medium Density Fiberboard (MDF) and Oriented Strand Board (OSB) models were in line with prior studies. Polyester batting & Polyester fabric have not been directly studied but their base polymer Polyethylene terephthalate (PET) has been studied however only two of the cited studies actually provided a pyrolysis model of a three-step reaction mechanism [22] and a two-step reaction mechanism [17]. The pyrolysis model presented for polyester batting & polyester fabric in this study is in line with the observations in the above studies. The reaction kinetic properties using the reaction mechanism were used to populate the 0-D milligram scale FDS model. The normalized mass curve and the mass loss rate curves were compared against the experimental data and they aligned with it depicting a good fit which generated confidence in the presented mechanisms. Other properties such as thermal conductivity and heat capacity were measured at room temperature which were then used to extrapolate the quantities for the complete temperature program Heats of reaction and heat of combustion for the materials were determined and combined with other properties, were used to populate the one-dimensional cone FDS model. The condensed phase solver in FDS which uses minimum computational power was used to carry out the simulations

thereby verifying its effectiveness with the solver. Since the gas phase solver was not invoked in modeling, to mimic the test conditions of flame heat feedback, empirical flame heat feedback model that has been developed was employed in the model. Cone testing for all materials at three different heat fluxes of 25 kW m^{-2}, 50 kW m^{-2} and 75 kW m^{-2} were conducted, and the model predictions of heat release rates were compared against the experimental cone data. For MDF and OSB at the lower heat flux, model predicted the first peak correctly but overestimated the peak heat release rate while the second peak was predicted early in time, but the peak heat release rate matched that of the second peak. This was hypothesized to be an effect of temperature dependent thermal conductivity and heat capacity, and the heat of reaction. It was also exaggerated by the flame heat feedback model that was employed which was provided credence by the predicted heat release rate curves for higher heat fluxes of 50 kW m^{-2} & 75 kW m^{-2}. For polymer materials the flame heat feedback application did not provide a good fit due to the materials having low thermal inertia, being thermally thin (polyester fabric) and absence of thermally dependent properties as well as the physical and thermal properties after phase change.

Additionally, the flame heat feedback is hypothesized to be a reason for non-conformance of model predictions since the model was developed using materials with high thermal inertia as compared to PU foam, polyester batting, and polyester fabric in this study. This aspect of the flame heat feedback model

combined with measurement of temperature dependent and phase change related properties needs to be revisited and verified with future work.

The study conducted on theses 5 materials provide an overview and an insight on testing of the rest of the materials planned in the project. The density input of the intermediates in the FDS model affects the output majorly specially for thermoplastic materials. The repeatability of the tests on the STA specially DSC are important to provide confidence (with lower uncertainties) while using the values, as well as reducing the number of parameters to revalidate. Specific heat measurement on the STA will provide the most accurate temperature and phase dependent specific heat values for use in the FDS model. Materials that tend to normally compress like polyester batting need to have the properties determined at the thickness which is most likely to be found in the built environment as it affects the density of the material. Clear outline and assumptions for kinetic analysis is important and decision between simplified mathematical kinetics and physically significant reaction mechanism needs to be made, for if they provide similar results within a range of uncertainty. A simplified mathematical kinetics with a higher reaction order makes sense for application in FDS modeling as it reduces the number of reactions and subsequently number of intermediates and determination of properties of each intermediate thereby reducing the time spent on modeling and complications associated with it.

A flame heat feedback application only FDS model should be validated with a 3-D gas phase simulation of the cone calorimeter which will provide an insight

on how the flame heat feedback model is affecting the computations in the condensed phase calculation. The smaller heat fluxes do not provide a good fit and improvements made for the smaller heat fluxes will provide robustness to data for use in global physical application. The gas phase simulation at the lab will provide the insight if developments can be made to the condensed phase + flame heat feedback model to make it more accurate and applicable in the field to reduce computational costs. Additionally, measuring the temperature profile of the sample throughout the cone tests can be determined and compared against the temperature profile generated from the FDS model to validate the model solution with the cone tests.

The next phase of study can involve the measurement of temperature dependent properties of the material. A step by step action would involve studying the effectiveness of the FDS model and flame heat feedback model for non-shrinking charring materials first. Then for the materials that tend to change phase before and during the pyrolysis need to have their phase changes properties determined. Once the properties are determined can be re-modeled in FDS to see where the model predictions stand with respect to experimental results. Additionally, the materials that generate multiple fuels can be modeled in layers in FDS and assigned different heats of combustions determined from experimental testing.

For FDS model to work effectively, the above properties need to be determined quantitatively. The cone calorimeter can be used to create polymer

melts to measure the density of the phase changed material as well as the properties of thermal conductivity and specific heat need to be measured. The Transient Plane Source (TPS) instrument at the lab has capabilities to find the thermal conductivity of the melts which can be utilized.

Another aspect of further study is conducting research on the oxidative pyrolysis. The STA experiments were conducted in an inert N_2 environment and the properties generated from it were used in the development of the model. There is a significant difference in the outcomes of the STA experiments when conducted in oxygen environment which changes the shape of the TGA mass loss curves due to interaction of various species differently in presence of oxygen [35][36]. As the cone calorimeter tests are conducted in an oxygen environment, the effect of properties developed from the oxidative pyrolysis process can be used to determine the properties and used to populate the FDS model to see the behavior of the model and compare it to the cone tests.

Fourier Transformed Infrared Spectroscopy (FTIR) instruments at the lab can be used to figure out the chemistry of the materials during pyrolysis. This can further help in estimating the material behavior at high temperatures after studying the pyrolysis products.

Bibliography

[1] USFA. Fire in the United States 2008-2017, 20th Edition. Report, Nov 2019

[2] The Fire Protection Research Foundation. *Recommendations of The Research Advisory Council on Post-fire Analysis*. White paper, Quincy, MA, 2002

[3] The Society of Fire Protection Engineers. *Research Needs for the Fire Safety Engineering Profession: The SFPE Roadmap*. White paper, 2018.

[4] Babrauskas, V. "Ignition Handbook", Fire Science and Technology Inc, Issaquah, WA." (2003).

[5] A.E. Cote, C.G. Grant, J.R. Hall, R.E. Solomon, and P.A. Powell, editors. *Fire Protection Handbook*. National Fire Protection Association, Quincy, MA, 20th ed. edition, 2008.

[6] M. Hurley, D. Gottuk, J.R. Hall, K. Harada, E. Kugliowski, M. Puchovsky, J. Torero, J.M. Watts, and C. Wieczorek, editors. *SFPE Handbook of Fire Protection Engineering*. Springer, Bethesda, MD, 5th ed. edition, 2016.

[7] UL FSRI. *Literature Review to Support the Development of a Database of Contemporary Material Properties for Fire Investigation Analysis.* Report, Columbia, MD, 2020

[8] Chattopadhyay, D. K., and C. Webster Dean. "Progress in Polymer Sci.–2009." V 34: 1068-1133.

[9] Herrera, M., et al. "Thermoanalytical and pyrolysis studies of nitrogen containing polymers." *Journal of Analytical and Applied Pyrolysis 58* (2001): 173-188.

[10] Wang, Pin-Sheng, et al. "Thermal degradation behavior and flammability of polyurethanes blended with poly (bispropoxyphosphazene)." *Polymer degradation and stability* 66.3 (1999): 307-315..

[11] Chao, Christopher YH, and Jing Hong Wang. "Comparison of the thermal decomposition behavior of a non-fire retarded and a fire retarded flexible polyurethane foam with phosphorus and brominated additives." *Journal of fire sciences* 19.2 (2001): 137-156.

[12] Rogers, F. E., and T. J. Ohlemiller. "Pyrolysis kinetics of a polyurethane foam by thermogravimetry; a general kinetic method." *Journal of Macromolecular Science—Chemistry* 15.1 (1981): 169-185.

[13] Bilbao, R., et al. "Kinetics of the thermal decomposition of polyurethane foams in nitrogen and air atmospheres." *Journal of Analytical and Applied Pyrolysis* 37.1 (1996): 69-82.

[14] Pau, Dennis SW, et al. "Determination of kinetic properties of polyurethane foam decomposition for pyrolysis modelling." *Journal of fire sciences* 31.4 (2013): 356-384.

[15] Garrido, María A., and Rafael Font. "Pyrolysis and combustion study of flexible polyurethane foam." *Journal of Analytical and Applied pyrolysis* 113 (2015): 202-215.

[16] Prasad, Kuldeep, et al. "Numerical simulation of fire spread on polyurethane foam slabs." *Fire research division, BFRL, NIST annual fire conference*. 2009.

[17] Martín-Gullón, I., M. Esperanza, and R. Font. "Kinetic model for the pyrolysis and combustion of poly-(ethylene terephthalate)(PET)." *Journal of Analytical and Applied Pyrolysis* 58 (2001): 635-650.

[18] Das, Pallab, and Pankaj Tiwari. "Thermal degradation study of waste polyethylene terephthalate (PET) under inert and oxidative environments." *Thermochimica Acta* 679 (2019): 178340.

[19] Girija, B. G., R. R. N. Sailaja, and Giridhar Madras. "Thermal degradation and mechanical properties of PET blends." *Polymer Degradation and stability* 90.1 (2005): 147-153.

[20] Yang, J., R. Miranda, and C. Roy. "Using the DTG curve fitting method to determine the apparent kinetic parameters of thermal decomposition of polymers." *Polymer Degradation and Stability* 73.3 (2001): 455-461.

[21] Nejman, Alicja, et al. "Thermal stability of polyester fabric with polyacrylic coatings." *Fibres & Textiles in Eastern Europe* (2015).

[22] Lautenberger, Chris, et al. "The role of decomposition kinetics in pyrolysis modeling-application to a fire retardant polyester composite." *Fire Safety Science* 9 (2008): 1201-1212.

[23] https://sailrite.wordpress.com/tag/how-to-add-batting-to-cushion-foam/

[24] https://www.shutterstock.com/image-photo/fabric-texture-433309222

[25] https://www.addicted2decorating.com/mdf-vs-plywood-differences-pros-and-cons-and-when-to-use-what.html

[26] https://www.designingbuildings.co.uk/wiki/Oriented_strand_board

[27] Vermesi, Izabella, et al. "Ignition and Burning of Fibreboard Exposed to Transient Irradiation." *Fire Technology* (2020): 1-19.

[28] Sinha, Arijit, John A. Nairn, and Rakesh Gupta. "Thermal degradation of bending strength of plywood and oriented strand board: a kinetics approach." *Wood science and technology* 45.2 (2011): 315-330.

[29] Li, Kai-Yuan, et al. "Pyrolysis of medium-density fiberboard: optimized search for kinetics scheme and parameters via a genetic algorithm driven by Kissinger's method." *Energy & fuels* 28.9 (2014): 6130-6139.

[30] Fateh, Talal, et al. "Kinetic and mechanism of the thermal degradation of a plywood by using thermogravimetry and Fourier-transformed infrared spectroscopy analysis in nitrogen and air atmosphere." *Fire safety journal* 58 (2013): 25-37.

[31] Aslan, Dilan Irmak, et al. "Thermokinetic analysis and product characterization of Medium Density Fiberboard pyrolysis." *Bioresource technology* 258 (2018): 105-110.

[32] Yang, Wenxu. *Pyrolysis and combustion properties of selected structural fuels in residential buildings*. Diss. MS Thesis, University of North Carolina at Charlotte, Charlotte, NC. Online access: https://ninercommons. uncc. edu/islandora/object/etd% 3A1637, 2016.

[33] Gong, Junhui, et al. "Development of a pyrolysis model for oriented strand board. Part I: Kinetics and thermodynamics of the thermal decomposition." *Journal of Fire Sciences* (2021): 0734904120982887.

[34] Yuen, Anthony Chun Yin, et al. "Establishing pyrolysis kinetics for the modelling of the flammability and burning characteristics of solid combustible materials." *Journal of fire sciences* 36.6 (2018): 494-517.

[35] McKinnon, Mark B., and Stanislav I. Stoliarov. "Pyrolysis model development for a multilayer floor covering." *Materials* 8.9 (2015): 6117-6153.

[36] McKinnon, Mark B., et al. "Pyrolysis model for a carbon fiber/epoxy structural aerospace composite." *Journal of Fire Sciences* 35.1 (2017): 36-61.

[37] McCoy, Conor G., Jessica L. Tilles, and Stanislav I. Stoliarov. "Empirical Model of flame heat feedback for simulation of cone calorimetry." *Fire Safety Journal* 103 (2019): 38-48.

[38] ASTM International. *D7309-20 Standard Test Method for Determining Flammability Characteristics of Plastics and Other Solid Materials Using Microscale Combustion Calorimetry*. West Conshohocken, PA; ASTM International, 2020.

[39] Lyon, R. E., et al. "Principles and practice of microscale combustion calorimetry." *Federal Aviation Administration* (2013).

[40] Lowden, Laura Anne, and Terence Richard Hull. "Flammability behaviour of wood and a review of the methods for its reduction." *Fire science reviews* 2.1 (2013): 1-19.

[41] Tleoubaev, Akhan, and Andrzej Brzezinski. "Thermal Diffusivity and Volumetric Specific Heat Measurements Using Heat Flow Meter Instruments for Thermal Conductivity 29/Thermal Expansion 17 Conference." *Thermal Expansion* 17.

[42] ASTM International. *E903-20 Standard Test Method for Solar Absorptance, Reflectance, and Transmittance of Materials Using Integrating Spheres*. West Conshohocken, PA; ASTM International, 2020

[43] ASTM International. *E408-13(2019). Standard Test Methods for Total Normal Emittance of Surfaces Using Inspection-Meter Techniques. Standard*. West Conshohocken, PA, 2019

[44] McKeen, Philip, and Zaiyi Liao. "Pyrolysis model for predicting the fire behavior of flexible polyurethane foam." *Building Simulation.* Vol. 12. No. 2. Tsinghua University Press, 2019.

[45] Atreya, Arvind, et al. "The effect of size, shape and pyrolysis conditions on the thermal decomposition of wood particles and firebrands." *International Journal of Heat and Mass Transfer* 107 (2017): 319-328.

[46] Tleoubaev, Akhan. (2007). Measurements of the Volumetric Specific Heat Cρ Using the FOX Heat Flow Meter Instruments.

[47] McGrattan, Kevin, et al. "Fire dynamics simulator user's guide." *NIST special publication* 1019.6 (2013).